Quantitative localization of $GABA_A$ receptor subunits on hippocampal pyramidal cells by SDS-digested freeze fracture replica labeling (SDS-FRL)

KASUGAI, Yu

DOCTOR OF PHILOSOPHY

Department of Physiological Sciences
School of Life Science
The Graduate University for Advanced Studies

2005

CONTENTS

1. ABSTRACT 2

2. INTRODUCTION 4

3. MATERIAL AND METHODS 11

4. RESULTS 18

5. DISCUSSION 30

6. LITERATURE CITED 39

7. FIGURES AND TABLES 48

8. ACKNOWLEDGEMENTS 68

1. ABSTRACT

The γ-aminobutyric acid (GABA) type A ($GABA_A$) receptors are the member of the ligand-gated ion channel superfamily mediating the majority of fast synaptic inhibition in the mature mammalian central nervous system. Pyramidal cells in the hippocampal CA1 area express 14 subunits of the $GABA_A$ receptor. The pyramidal cells receive input from various interneurons such as basket cells, bistratified cells and axo-axonic cells, which make synapses on the soma, dendrite and axon initial segment (AIS), respectively. Here, we used SDS-digested freeze-fracture replica labeling (SDS-FRL) method to visualize two-dimensional distribution of α1, α2 and β3 receptor subunits quantitatively on the distinct subcellular compartments of pyramidal cells. The SDS-FRL method provides two-dimensional distribution maps of membrane molecules. Immunogold particles for these subunits were accumulated over clusters of intramembrane particles (IMP) on the protoplasmic face (P-face) of the plasma membrane, indicating that the IMP clusters represent GABAergic synapses in replica. On the somata, the synaptic areas obtained were 0.051 ± 0.022 μm^2 (mean ± SD, n=54) in the sample labeled for β3, 0.053 ± 0.038 μm^2 (n=61) for α1 and 0.041 ± 0.022 μm^2 (n=70) for α2. The sizes of labeled synapses in the four samples were not significantly different, indicating a consistent delineation of synaptic areas. The synaptic areas in dendrites were 0.049 ± 0.025 μm^2 (mean ± SD, n=35) in the sample labeled for β3, 0.058 ± 0.044 μm^2 (n=33) for α1 and 0.037 ± 0.037 μm^2 (n=72) for α2. These values were also not significantly different between each other and from those in the soma. However, the synaptic areas in AIS (0.011 ± 0.015 μm^2 for β3, 0.014 ± 0.007 μm^2 for α2) were significantly smaller than those in the soma and dendrite.

The densities of immunogold particles for the β3 subunit in the synaptic area were 904.81 ± 682.08 (No/μm^2, mean ± SD, n=54) in soma, 863.08 ± 542.32 (n=35) in apical dendrite, and 704.02 ± 254.09 (n=4) in AIS. The densities of synaptic β3 labeling were not

significantly different in the three compartments. The labeling densities for the α1 subunit were 212.25 ± 96.41 (No/μm^2, mean ± SD, n=61) in soma and 220.82 ± 113.9 (n=33) in apical dendrite, and those for the α2 subunit were 592.23 ± 267.02 (No/μm^2, mean ± SD, n=70) in soma, 642.63 ± 269.20 (n=72) in apical dendrite, and 601.78 ± 245.45 (n=9) in AIS. The synaptic labeling densities for the α subunits were also not significantly different between these compartments.

Extrasynaptic labeling densities for the β3, α1 and α2 subunit were about 1/100th of synaptic labeling, but 10 times higher than background density of particles, suggesting that a significant proportion of $GABA_A$ receptors is localized at the extrasynaptic membrane of the pyramidal cell soma.

To examine co-localization of different $GABA_A$ subunits in single synapses on soma, double labeling with two kinds of antibodies was performed. The double labeling experiments with α1, α2 and β3 subunit specific antibodies indicated that 80% of β3 positive GABAergic synapses on soma include α1 or α2 subunits. Conversely, almost all of the α subunit positive synapses were β3 positive. Furthermore, α1 and α2 subunits are almost always co-localized in the same synapses, indicating that about 20% of β3 positive synapses are negative for both α1 and α2.

The present findings indicate that α subunit expression in pyramidal cell synapses in different subcellular compartments are more homogeneous than previously reported. The present study also revealed subpopulations of somatic GABAergic synapse with distinct α subunit expression, which may be differently affected by subunit selective ligands.

2. INTRODUCTION

Since Scoville and Milner introduced a paper in 1957, the hippocampus is one of the most studied regions of mammalian central nervous system (CNS). The authors showed the neuropsychological findings from a patient whose initials are H.M. in the paper (Scoville and Milner, 1957). The patient underwent removal of bilateral hippocampus for the treatment of epilepsy, to suffer a permanent loss of the ability to encode new information into long-term memory. Similar memory-impairment has been seen in other patients with bilateral damage restricted to the hippocampus (Zola-Morgan et al., 1986). These cases suggest strongly that hippocampus is necessary for certain forms of memory. Moreover, recent three decades of research conducted in rodents have demonstrated that neurons in the hippocampus are preferentially activated by certain stimuli located in the environment.

The hippocampus *in vitro* and *in vivo* displays very characteristic rhythmic synchronized activities, and those rhythmic network activities are also evidenced as oscillations in the extracellularly recorded field potential. These oscillations have been hypothesized to serve various complex functions, such as perception, cognition, movement initiation and memory (O'Keefe and Recce, 1993; Wilson and McNaughton, 1993; Bragin et al., 1995; Skaggs et al., 1996), and these firing patterns of pyramidal cells are modulated by a diverse population of GABAergic interneurons (Bragin et al., 1995; Whittington et al., 1995; Freund and Buzsaki, 1996; Fisahn et al., 1998; Csicsvari et al., 1999; Klausberger et al., 2003; Mann et al., 2005).

Since Whittington et al. showed that $GABA_A$ receptor-mediated inhibition between interneurons induces gamma-oscillation in hippocampus (Whittington et al., 1995), it has been clear gradually that GABAergic inputs can synchronize the firing of pyramidal cells

generating network activities at theta and gamma frequencies, and that GABAergic interneurons and their inhibitory synapses play a major role in these oscillatory patterns throughout the hippocampus (Freund and Buzsaki, 1996; Csicsvari et al., 1999; Klausberger et al., 2003; Mann et al., 2005; Somogyi et al., 2005).

The hippocampus consists of 80-90% of glutamatergic pyramidal neurons and only about 10% GABAergic interneurons (Freund and Buzsaki, 1996), but single hippocampal inhibitory cells innervate hundreds of pyramidal cells (Sik et al., 1995), so the output of a single interneuron can produce periodic inhibition synchronizing the firing of spontaneously active pyramidal cells (Cobb et al., 1995). Hippocampal pyramidal cells receive on soma and dendrites, thousands of inhibitory synaptic inputs at many locations, which originate from several distinct populations of interneurons. These interneurons show domain–specific innervation of pyramidal cells (Freund and Buzaki, 1996; Somogyi et al., 1998), e.g., axo-axonic cells innervate only the axon initial segment (AIS), parvalbumin (PV) or cholecystokynin (CCK) containing basket cells innervate the soma and the proximal dendrites, other interneurons (i.e., bistratifeid cells) innervate only the dendrites of pyramidal cells (Kosaka T., 1980; Somogyi et al., 1983; Lacaille and Schwartzkroin, 1988; Gulyas et al., 1993; Mcbain et al., 1994; Buhl et al., 1994). Therefore the spatial segregation of terminals of interneuron on pyramidal neurons suggests functional specialization among GABAergic interneurones: dendritic projecting interneurons, which control the input of principal cells, and interneurons that selectively innervate the soma of pyramidal cells, which control the output of principal cells (Miles et al., 1996). Accordingly it is very important to know the feature of GABAergic synapses on pyramidal cell, for understanding property of pyramidal cell as "neuronal elemental device in hippocampus".

The γ-aminobutyric acid (GABA) type A ($GABA_A$) receptors are the member of the ligand-gated ion channel superfamily mediating the majority of fast synaptic inhibition in

the mature mammalian central nervous system. They are permeable to Cl^- and to a less extent HCO_3^-. The conformational changes (Horenstein et al., 2001) caused by the binding of GABA open the channel and the influx of chloride ions according to their electrochemical gradient results in hyperpolarisation of the postsynaptic membrane, hindering the spread of excitability. These receptors also have sites of action of many drugs in wide clinical use; these include ligands of the benzodiazepine site of the $GABA_A$ receptor, barbiturates (Sieghart, 1995). Therefore $GABA_A$ receptors are important in neuropharmacology, and a major goal in neuropharmacology has been to target drugs selectively to defined $GABA_A$ receptor subtypes and refine the therapeutic spectrum of the presently available drugs, reduce their side-effects and discover new therapeutic indications.

Molecular cloning studies in mammals have resulted in the identification of a lot of $GABA_A$ receptor subunit families [α(1-6), β(1-3), γ(1-3), ρ(1-3), δ, ε, π, and θ] , encoded by a separate genes (Sieghart, 1995; Davies et al., 1997; Hedblom and Kirkness, 1997; Hevers and Luddens, 1998; Watanabe et al., 2002). Each receptor polypeptide has been classified purely on the basis of sequence identity, with subunits being attributed to particular classes (i.e., α, β, or γ) (Davies et al., 1997). The $GABA_A$ receptors are transmembrane heterooligomeric proteins composed of five homologous subunits (Tretter et al., 1997; Fritchy and Brunig, 2003), and those receptors also possess a pentameric structure (Nayeem et al., 1994; Baumann et al., 2001, 2002). Recombinant $GABA_A$ receptors can be assembled from differential combinations of the subunits (Sieghart, 1995; Moss and Smart, 2001). These facts arise the question, "What is the functional significance of these molecular diversity expressed in various CNS neural circuits for the GABAergic inhibition of neuronal membrane excitability?" The experiments using subunit specific antibodies to immunoprecipitate native receptor molecules, immunohistochemical mapping of individual subunits and expressing combinations of subunit cDNAs in mammalian cells have suggested that a more finite number of $GABA_A$ receptor subtypes exist in the brain. It

is generally accepted that most receptors possess 2 α subunits, 2 β subunits, and 1 γ subunit (Chang et al., 1996; Baumann et al., 2002). The precise subunit composition of native $GABA_A$ receptors on the surface of neuron is not well determined, because the stoichiometry of the $GABA_A$ receptors is highly variable in different brain regions and the same channel can include more than one α or β subunit species (Pritchett et al., 1989; Benke et al., 1996; Sperk et al., 1997).

Pharmacological profiles and features of $GABA_A$ receptor depend on the subunits included. $GABA_A$ receptor containing α1, α2, α3 and /or α5 are equally sensitive to broad spectrum agonists, but high affinity for benzodiazepine type 1 agonists, e.g. Zolpidem requires α1. Benzodiazepine type 1 receptors are therefore those that contain an α1 subunit, while type 2_M receptors contain α2 or α3 subunits, and type 2_L receptors contain α5 subunits (Ruano et al., 1992; Benavides et al., 1993; Sieghart, 1995; Johnston, 1996; Johnston, 2005). Moreover 2 different α subunits can co-exist in a single $GABA_A$ receptor from rat whole brain (Duggan et al., 1991; Pollard et al., 1993) and in the hippocampus (Araujo et al., 1999). These co-existences make the feature of $GABA_A$ receptors complicated, for example, the α1 subunit co-assembled with the α3 subunit displayed predominantly type 1 benzodiazepine binding sites (Araujo et al., 1996).

Immunohistochemistry and *in situ* hybridization studies indicate that the distribution of $GABA_A$ receptor subunit can differ among brain regions (Persohn et al., 1992; Wisden et al., 1992; Sperk et al., 1997; Pirker et al., 2000), especially in cortical regions, such as hippocampus, where synaptic inhibition has been extensively studied. Within the hippocampal formation, five α subunits (α1-α5) were shown to be expressed at mRNA level. At the protein level, α1, α2 and α5 subunits are the most abundant subunits, whereas α3 and α4 subunits are weakly expressed. Although mRNAs of all the three β subunits are expressed in the hippocampal pyramidal layer, β1 and β3 subunits are the most prominently translated proteins. The subcellular distribution of the α1, α2, β2/3 and γ2

subunits have been studied at the synaptic level on ultrathin sections (Nusser et al., 1996; Somogyi et al., 1996; Nyiri et al., 2001; Klausberger et al., 2002). It is not clear whether α5 is localized in synapse or not, and their studies are done only in cultural cells, not in tissues (Brunig, et al., 2002; Christie and Blas, 2002).

Nusser et al. (1996) demonstrated that α1 and α2 subunits have a differential distribution in synapses in hippocampal pyramidal cells. The α1 subunit was found evenly distributed in GABAergic synapses throughout cell compartments (soma, dendrite and axon-initial segments), whereas the α2 subunit was selectively concentrated in synapses on the axon-initial segments (AIS). Furthermore, immunofluorescence in brain sections by microwave irradiation revealed obvious specificity in the synaptic targeting of $GABA_A$ receptor subunits and confirmed the prominent α2 subunit staining in AIS (Fritschy et al., 1998; Brunig et al., 2002). While α1 and α2 subunits are main α subunits of synaptic $GABA_A$ receptors in the CA1 and CA3 regions of the hippocampus, $GABA_A$ receptors with α5 subunit are localized primarily to extrasynaptic regions of pyramidal cell (Crestani et al., 2002; Brunig et al., 2002; Houser and Esclapez, 2003). These studies suggest that the distribution of $GABA_A$ receptor subunit can differ not only among regions and cells, but also among different cellular compartments.

Therefore the spatial segregation of terminals of interneuron on pyramidal neurons and the different subunit composition of $GABA_A$ receptors among cellular compartments provide a possibility. The possibility is that presynaptic factors control the subunit composition of postsynaptic receptors, however, little is known about the signals controlling subcellular targeting of $GABA_A$ receptors. Some studies support the hypothesis on hippocampal pyramidal cell somata. Immunoreactivity for the α2 subunit was stronger in synapses formed by PV-negative boutons than in synapses formed by PV-positive boutons (Nyiri et al., 2001). Reversely, synapses innervated by PV-negative boutons on pyramidal cell somata have a lower density of α1 subunits than synapses innervated by

PV-positive boutons (Klausberger et al., 2002).

As described above, subunit–compositions of $GABA_A$ receptors are of great variety, and itself is important for function of hippocampus, and density of each $GABA_A$ subunit in a synapse between cellular compartments is also meaningful. In present study, we measured the density of each $GABA_A$ subunit, $\alpha 1$, $\alpha 2$ and $\beta 3$ in synapse and extrasynapse and examined the ratio of co-localization of each α subunit in a single synapses by "SDS-digested freeze-fracture replica labeling method (SDS-FRL)".

The freeze-fracture technique was first introduced as a technical concept in 1950 (Hall. 1950). It can reveal the macromolecular architecture of the membrane interior, the distribution of a wide variety of transmembrane macromolecules as intramembrane particles (IMPs) as two-dimensional distribution. However, the conventional freeze-fracture technique can't offer direct information on the biochemical composition of membrane components. Freeze-fracture cytochemistry, which is the combination of freeze-fracture with cytochemical labeling of individual cell membrane molecules, provided direct evidence of the chemical nature and topology of the cell membrane components (Takizawa and Saito, 1996; Torris and Mancini, 1996). However, this technique has also limitations, because it can label only outer membrane halves of monolayers, and it is not applicable to complex tissue, such as brain.

SDS-FRL is developed from freeze-fracture technique to solve those limitations (Fujimoto, 1995). SDS can dissolve not only unfracturred membrane and cell components, but also proteins masking objective intramembrane proteins; this technique can detect molecules in dense matrix. For example, Hagiwara demonstrated that t-SNARE proteins exist at the presynaptic active zone (Hagiwara et al., 2005). No clear immunoreactivity for t-SNARE proteins had been demonstrated at the active zone so far by conventional preembedding immunocytochemistry. Unmasking by digestion with SDS can exclude dense matrix associated with cell membrane, so it increases accessability of antibody, and

in consequence, sensitivity for the antibodies. Immunoreaction of SDS-FRL is similar to that of SDS-PAGE in principle, SDS denatures proteins by unfolding their secondary, tertiary and quaternary structures. Their antigenicity can be kept, but the replicated membrane itself has information of membrane-structure and localization of proteins. SDS-FRL is also able to show cell membrane as two-dimensional plane and visualize two-dimensional distribution of integral membrane proteins using site-directed antibodies. When synaptic area is observed, extrasynaptic area is examined at the same instant too. It is an advantage to compare labeling density of synaptic and extrasynaptic sites.

In the present study, I used SDS-FRL to investigate quantitatively labeling density of the $GABA_A$ subunit $\alpha1$, $\alpha2$ and $\beta3$, in the synaptic and extrasynaptic subcellular compartments, the soma, dendrite and AIS. Glutamatergic synapses have been demonstrated already by SDS-FRL (Tanaka et al., 2005), GABAergic synapses, however, have not yet well identified. So I first tried to define GABAregic synapses on replicas, and I indicated combination of IMP-clusteres and $GABA_A$ subunit labeling is useful for identification of GABAergic synapses on hippocampal pyramidal cells. Since SDS-FRL has about 4 times sensitivity than conventional postemmbedding immunocytochemistory, I could demonstrate detailed synaptic/extrasynaptic ratio on each cellular compartment. Synaptic labeling densities on each cellular compartments were not significantly different for each subunit, and synaptic labeling densities were 100 times higher than extrasynaptic labeling densities. Combined labeling for α subunits and $\beta3$ subunit showed that 80% of $\beta3$ positive synapses have $\alpha1$ or $\alpha2$ positive synapses mostly have with $\beta3$.

These results suggest that different from present hypothesis, $\alpha1$ and $\alpha2$ subunits are evenly distributed in different subcellular compartments and revealed subpopulation of somatic GABAergic synapses with distinct α subunit combinations.

3. MATERIAL AND METHOD

Preparation of primary antibodies

Dr. Sieghart kindly gave us plasmids for GST-fusion proteins with $GABA_A$ α1 and β3 subunits. Both plasmids include portions of the intracellular loop corresponding to residues 328-382 of α1 subunit and residues 345-408 of β3. I developed guinea pig and rat polyclonal antibodies using GST-fusion proteins derived from those plasmids. For immunization, these fusion proteins were purified by sodium dodecyl sulphate-polyacrylamide gel electrophoresis (SDS-PAGE) method. After electrophoresis, the gels were washed briefly in several changes of deionized water and then transferred to 0.3 M $CuCl_2$. After shaking gently the gel for 3 min, broad bands appeared in the gel against a black background, and were excised from the gel using a razor. The gel fragments containing the purified fusion protein were emulsified with Freund's adjuvant (Nakalai tesque, Kyoto, Japan), and 50-100 μg fusion protein was injected into guinea pigs per animal, and 20-50 μg fusion protein into each rat. The following immunizations were done in incomplete Freund's adjuvant at 4-week intervals. The antisera were collected 2 weeks after the second injection.

Primary antibodies

Full antisera and the purified antibodies were used. The antisera are to subunits $GABA_A$ α1 (1/50; developed in rat), β3 (1/50; developed in guinea pig), and purified antibodies are to subunit $GABA_A$ α2 polyclonal antibody from rabbit (1/900; kindly provided by Dr. Sieghart), to Nav1.6 monoclonal antibody from mouse (1/500; kindly provided Dr. Trimmer) and to Nav1.6 polyclonal antibody from rabbit (1/1000; Alomone labs, Jerusalem, Israel).

Tissue for immunohistochemistry

Eight adult male Wister rats, 8 weeks of age, were used in the present study. All animal experiments were conducted in accordance with the National Institute for Physiological Science's Animal Care and Use Committee. Rats were deeply anesthetized with sodium pentobarbital (50 mg/kg, i.p.) and perfused transcardially with 25 mM PBS (Phosphate-Buffered Salines) for 3 min, followed by 2% paraformaldehyde and 15% picric acid in 0.1 M phosphate buffer (PB, pH 7.3-7.4) for 12 min and followed by 25 mM PBS for 3 min again. The brains were removed immediately, and washed in PBS at 4 ℃.

Light microscopic immunohistochemistry

Sections (50 μm thick) containing the hippocampus were cut with a Lineaslicer PR7 (Dosaka EM, Kyoto, Japan). After washing in 25 mM PBS and blocking in Primary antibody solution (PBS containing 0.1% Triton X-100, 0.25% λ-carageenan and 0.5% normal goat serum) containing 10% normal goat serum (NGS), sections were incubated with primary antibody in the Primary antibody solution for over night at 4 ℃. After washing, the sections were incubated with biotinylated secondary antibodies (1:200, Vector, CA, USA) at room temperature for 2hr and then with avidin-biotin peroxidase complex (1:100 ABC-Elete; Vector) at room temperature for 1hr. Subsequently, the sections were incubated in 50nM Tris-HCl (pH 7.4) containing 0.025% 3-3-diaminobenzidine tetrahydrochloride (DAB; Nakalai tesque, Kyoto, Japan) and 0.003% hydrogen peroxide. The sections were washed in several times with PBS, dehydrated with graduated EtOH and mounted on slide-glasses with Mount-Quick (mounting media; Daido-sangyo, Saitama, Japan). The slides were examined with BX50 light microscope (OLYMPUS, Tokyo, Japan), and the images were digitalized through DP70 digital camera (OLYMPUS, Japan).

Cell culture and transient transfection procedures

We received plasmids including cDNA for $GABA_A$ receptor α subunits (α1, α2 and

α5), cloned into a pCl vector, β subunits (β1, β2 and β3) and the γ2 subunit from Dr. W. Sieghart. The pCI vector utilized the cytomegalovirus immediate-early enhancer/promoter region for strong constitutive expression of the αA gene. When expressed, the proteins include complete sequences of each subunit. We cultured human-derived renal epithelial HEK-293 cells provided by Dr. J. McIlhinney (MRC, Anatomical Neuropharmacology Unit, Oxford University, UK). The cells were grown and subcultured in Dalbecco's Modified Eagle's Medium (DMEM) supplemented with 2.5% fetal bovine serum (FBS), glutamine (0.29 g/l), sodium bicarbonate (2.2 g/l), penicillin (100,000 U/l), and streptomycin (10 mg/l) in an atmosphere of 5% CO_2-95% air at 37 ℃. The HEK-293 cells were grown for approximately 15 hours in 6 well plates on glass coverslips coated with p-lysine and seeded with 0.5 X 10^6 cells per a well. Transient transfection by the plasmids was carried out using FuGENE6 (Roche Applied Scince). In each well, 0.5 μg plasmid was applied for single trasfections in a volume of 25 μl. For double or triple transfections, the amount of DNA was twice or thrice that amount and the FuGENE6 solution also doubled or tripled. The DNA solution was mixed with the FuGENE6 solution at a ratio of 1:6 (DNA:FuGENE), and 3.5 μl of this solution was added to serum free DMEM, to a volume of 200 μl and kept for 20 minutes at room temperature. Before transfection, the medium on the cells was changed to a fresh medium and incubated for 30 minutes. Transfection was initiated by adding 200 μl of the above medium containing DNA to each well. The cells were grown for 48 hours before fixation.

Imunohistchemistry for $GABA_A$ receptor subunits in HEK cells

The transfected cells were fixed with 4% paraformaldehyde (PFA) and 15% (v/v) picric acid dissolved in 0.1M PB (pH 7.4) for 30 minutes at room temperature. The fixed cells were washed 3 times in 0.1M PB for 5 minutes. Blocking non-specific antibody binding was carried out with 20% normal horse serum (VECTOR, Burlingame, CA) in 0.3% Triton X-100 and TBS (TBS-T) for 1 hour. Primary antibodies were applied in 1%

NHS in TBS-T for 2 hours at room temperature. For multiple-labeling experiments, several primary antibodies were incubated simultaneously. After washing, the cells were incubated with secondary antibodies. For simultaneous detection of different primary antibodies, Alexa Fluor-488 goat anti-rabbit IgG (1:1000; Molecular Probes), Cy3-coupled anti-guinea pig (1:400; Jackson ImmunoResearch Europe Ltd., Cambridgeshire, UK) and Cy5-coupled anti-rabbit, anti-guinea pig or anti-rat (1:400; Jackson ImmunoResearch Europe Ltd.) subtype- and species-specific secondary antibodies were used. Secondary antibodies were diluted with TBS-T, and reacted for 1 hour at room temperature. After 2 times washing with TBS-T and once washing with TBS, the cells on glass coverslip were covered with Vectashield (VECTOR) anti-fading medium. Fluorescence images were captured with a Digital CCD camera C4742-95-12 NRB (HAMAMATSU, Japan) on a LEITZ DM RB microscope (Leica) with epifluorescence illumination equipped with the following filter blocks: A4 (excitation filter BP 360/40 nm, reflection short pass filter 400 nm, suppression filter BP 470/40 nm), L5 (excitation filter BP 480/40 nm, reflection short pass filter 505 nm, suppression filter BP 527/30 nm), Y3 (excitation filter BP 545/30 nm, reflection short pass filter 565 nm, suppression filter BP 610/75 nm), and Y5 (excitation filter BP 620/60 nm, reflection short pass filter 660 nm, suppression filter BP 700/75 nm). Image processing was carried out with the software Openlab (Improvision Ltd., Coventry, UK).

Freeze-fracture immunolabeling

Fixed brains were removed from rats and washed in PBS for 30 min. Subsequently the brains were cut coronally with a Lineaslicer PR7 (Dosaka EM, Kyoto, Japan) with 100 μm thickness. The sections including hippocampal CA1 area were cryoprotected with 30% glycerol in 0.1 M PB for over night at 4 ℃, and were quickly frozen on pairs of gold hats carrier by a high pressure freezing machine (HPM010; BAL-TEC, Balzers, Liechtenstein). Frozen samples were inserted into double replica table and then fractured into two sections at -115 ℃. Fractured faces were replicated by deposition of carbon (5 nm thickness),

platinum (uni direction from 60°; 2 nm thickness), and carbon (20 nm thickness) in freeze-fracture replica machine (BAF 060; BAL-TEC). After bringing out the samples from the machine, tissue with replica were washed in PBS. For SDS-digestion, the replicas were incubated in 800μl digestion solution (15 mM Tris-HCl buffer (pH 8.3), 2.5% SDS and 20% sucrose) at 105 ℃ for 13 min in autoclave (Lab Autoclave MLS-3020, SANYO, Osaka, Japan) and kept for about 5 hr till the temperature in the chamber fall in room temperature.

The digested replicas were washed by TBS (Tris-Hcl-Buffered Salines) containing 0.05% bovine serum albumin (BSA; Nakalai tesque), and blocked by antibody solution containing 5% BSA in TBS for 30 min. Sequentially the replica was put in the antibody solution containing primary antibodies at 4 ℃ for over night. After a few washes with 0.05% BSA in TBS, the replicas were reacted in secondary antibodies conjugated with gold particles (GE Healthcare Bio-Sciences, Piscataway, USA or British Biocell International, Cardiff, UK) for 2 hr in a incubator (MIR-162, SANYO) at 37 ℃. After several washes with 0.05% BSA in TBS and distilled water, the replicas picked onto 75-mesh cupper grids (Pelco, USA). Electron microscopy was done using an EM208S transmission electron microscope (PHILIPS, Netherlands).

For double sequential labeling, the antibody to be measured quantitatively was reacted at first, the secondary antibody for the first primary antibody was applied, the second primary antibody was reacted sequentially, and then the second secondary antibody was applied. The secondary antibody for the first primary antibody was conjugated with 5 nm gold particle, and the secondary antibody for the second primary antibody was conjugated with 10nm gold.

Testing the specificity of antibodies on freeze-fracture replicas from gene knock out mice

Mice with a disrupted gene of the $GABA_A$ α1 (Sur et al., 2001) and wild type

littermates were obtained from Drs. D. Belleli and J. Lambert at the Neurosciences Institute, University of Dundee. The mice were perfused by Dr. J. H. J. Huck in MRC Anatomical Neuropharmacology Unit (Oxford University, UK) the same way as in our laboratory at Okazaki, and replicas were prepared using BAF060 for fracturing and HPM010S for freezing the tissue. The procedure for SDS digestion and immunolabeling were the same as described above. A CM100 transmission electron microscope (PHILIPS, Netherlands) equipped with a Digital CCD camera Gatan Ultra Scan 1000 (Gatan,Inc., Pleasanton, CA, USA) was used to obtain data. Imaging processing was carried out with the image processing software Digital Micrograph (Gatan), and ImageJ softwere was used for measuring synaptic area.

The antiserum to the β3 subunit raised in guinea pig were tested on replicas of β3 KO mouse (source: Dr Thomas Rosahl, Merck Sharp & Dohme, The Neuroscience Research Centre, Terlings Park, Harlow, UK) along with littermate wild type mouse. Both animals were also tested for the α1 subunit with antibodies raised in rat.

Measurement of synaptic area and quantification of density of immunogold particles

Electron microscopic imageshs were printed on projection paper (Fujibro WP FM3; Fuji photo film, Tokyo, Japan). When IMP-clusters were taken in a picture, surrounding area was also taken in the same picture. Synapses were defined as 1) IMP-clusters with more than 5 IMPs (intramembrane particles), which were not separated more than 30 nm from the closet particle, and 2) IMP-clusters with at least two immunogold paricle at least. Area of synapse were defined by lines surrounding edge of IMP-clusters, and the area were measured by ScionImage (freely down loaded from from http://www.scioncorp.com/). Much the same is true on the surrounding area, extrasynapse. Only P-face of replicas were observed in the present study, because all used antibodies recognized intracellular domains. For calculating density of each labeling, number of 5 nm gold particles in synapse and extrasynapse were measured. Data for quantification were obtained from one Wister rat.

Statistical analysis was done by SPSS (SPSS, IL, USA).

Measuring synaptic area in ultra-thin sections from rats fixed with Karnovsky's fixative

Adult male Wister rats, 10 weeks of age, were used in this experiment. Rats were deeply anesthetized with sodium pentobarbital (50 mg/kg, i.p.) and perfused transcardially with 25 mM PBS (Phosphate-Buffered Salines) for 3 min, followed by 4% paraformaldehyde, 0.05% Gluteraldehyde and 15% picric acid in 0.1 M phosphate buffer (PB, pH 7.3-7.4) for 12 min and followed by 25 mM PBS. After perfusion, the brains were removed immediately, and kept in same fixative solution at 4 ℃ for overnight. Sections containing the hippocampus were cut with a Lineaslicer PR7 (Dosaka EM, Kyoto, Japan) at 50 μm thick. After washing in 0.1 M PB, the sections were fixed with 1% OsO_4 and 7% sucrose in 0.1M PB for 60 minutes at room temperature and reacted uranyl-acetate solution. And then the sections were dehydrated and embedded into Epoxy resin. The embedded sections were cut at 80 nm with ULTRACUT UCT (Leica).

Electron microscopy was done using a CM100 transmission electron microscope captured with a Digital CCD camera Gatan Ultra Scan 1000. Imaging processing was carried out with the image processing software Digital Micrograph. Synaptic length was measured with ImageJ (NIH).

4. RESULTS

Testing the specificity of primary antibodies

Antibodies to the intracellular loop of the α1, α2 and β3 subunits had been developed in rabbit by Sieghart et al., (Sieghart and Sperk, 2002), and were available for labeling one subunit at a time. Immunohistochemistry using these antibodies showed specific staining pattern in the hippocampus (Sperk et al., 1997). After producing fusion proteins, I developed antibodies to the intracellular loop of the α1 subunit and the β3 subunit in rats and guinea pigs, respectively. The anti-α1 antibody from rat and the anti-β3 antibody from guinea pig showed similar labeling patterns (Fig.1) to those previous results using the rabbit antibodies. The staining pattern for the α1 subunit was prominent within the hippocampal formation, and it was evenly distributed in dendritic areas of pyramidal cells in the CA1 and CA3 areas (Fig.1A). The cell body layers, stratum lucidum and the hilus were lightly stained. Some interneurons in all areas were more strongly labeled than neighboring pyramidal cells (Fig.1B). The immunolabeling with the antibody to the β3 subunits was also distributed throughout the hippocampus; the cell body layers, str. lucidum and the hilus were lightly labeled (Fig.1C), and it was similar to that reported previously (Sperk et al., 1997).

Antibody specificity as tested on transfected HEK cells

Next, cross-reactivity of antibodies was tested with transfected HEK cells. The results are summarized in Table A and Fig.2. All tested antibodies showed strong labeling of the cells transfected with the subunit containing the amino acid sequence to which the antibody was raised, but not the cell transfected with other subunits. Hippocampal pyramidal cells mainly express α1, α2 and α5 subunits as alpha subunit of $GABA_A$ receptors, therefore we tested these three subunits. All three β subunits have been reported

to be expressed by pyramidal cells, therefore we tested them all. Functional cell surface $GABA_A$ receptors in the brain consist of α, β and γ subunits and they may have different folding when assembled into a full receptor as compared to when expressed as single subunit. Therefore, we tried both co-expression of several subunits and single subunit expression, but we obtained the same results with regard to antibody specificity. The rat antibodies to the α1 and the guinea pig antibodies to the β3 subunits were used as full antisera at relatively high concentration, which may result in more non-specific labeling when applied to the replicas. However, on HEK cells they showed clear specificity for the α1 and β3 subunits only.

Morphological characteristics of pyramidal cells in the hippocampal CA1 replica

The hippocampus is an ideal area to study synaptic organization because of its clear lamellar structure (Anderson et al., 1971); the main laminae in the CA1 area being strata oriens, pyramidale, radiatum and lacunosum-moleculare (Fig 3A). The pyramidal cell bodies are located mainly in str. pyramidale, the basal dendrites in str. oriens, the apical dendrites with their oblique side branches in str. radiatum and the terminal tuft of the apical dendrite in str. lacunosum moleculare. When replicas were made from hippocampal slices, pyramidal cells could be identified as relatively large elliptical or triangular structures, and apical dendrite as radially extended large diameter processes often in continuity with cell bodies (Fig.3B). These structures were clear also under electron microscope (Fig.3C and 3D). So I could discriminate cell bodies and apical dendrites by their size, shape and location. Smaller dendrites and dendritic spines were also recognizable. However, it was impossible to recognize the AISs of pyramidal cells on the basis of their size or location in the hippocampal replicas, because their size and location overlaps with the basal dendrites. I was interested in the AIS because of its distinct GABAergic innervation by axo-axonic cells (Kosaka, 1980, Somogyi et al., 1983)

In freeze fracture replica literature the extracellular half of the plasma membrane is

called the E-face and the cytoplasmic or protoplasmic half the P-face. These can be recognized from the density of IMPs and curvature of the membranes. The P-face has a much higher density of IMPs than the E-face. The membrane of some cells, e. g. astroglial cells, can be recognized from characteristic structures as result of the expression of specific proteins, resulting in unique IMPs or IMP density. I searched the area where the AIS of pyramidal cells are located, but could not find a structural feature that would have enable me to identify AIS in replicas, therefore I needed a specific molecular marker for the AIS.

Identification of the AIS of pyramidal cells in the replica

Voltage-gated sodium channels (Navs), are present in excitable cells. In neuronal tissue, they are responsible for generating and propagating action potentials. Brain Navs are heteromers of $\alpha\beta_1\beta_2$ subunits and the α subunit forms the channel pore. The Nav1.6 α subunit is expressed in the somata of hippocampal pyramidal cells at mRNA level (Schaller et al., 2000) and at protein level (Donna et al., 2000). A commercial anti-Nav1.6 antibody showed strong expression of the protein not only in soma but also in radial thins structures corresponding to AISs in a dense band on the stratum oriens side of the pyramidal layer (Fig.3E). At higher magnification, individual AISs could be seen emerging from pyramidal cell bodies. This antibody also labeled radially oriented processes of a diameter expected of the AIS in the pyramidal layer and in st. oriens in SDS-FRL (Fig.3F). Therefore, I could use this antibody as an AIS specific marker. The ability to distinguish in replicas the soma, apical dendrite and the AIS, functionally distinct cellular compartments of the pyramidal cell, enabled me to compare their receptor composition. Because pyramidal cells express at least 14 distinct subunits of the $GABA_A$ receptor, I planned to study the distribution of several subunits simultaneously, which required specific antibodies to the different subunits raised in different host species.

GABAergic synapses revealed in SDS-FRL for $GABA_A$ receptors

Application of antibodies to the intercellular loop domain of $GABA_A$ receptors resulted in specific labeling on the expected P-face on CA1 pyramidal cells (Somogyi et al., 2004 Soc Neurosci Abst). The labeling was particularly dense over islands of dense IMP-clusters and majority such clusters were labeled. The frequency and size of these high-density IMP-clusters resembled the expected distribution and size of GABAergic synapses. However, not all IMP-clusters were labeled for $GABA_A$ receptor subunits and most of the non-clustered IMPs on the P-face were not immunolabeled (Fig.4A). Therefore, I compared the size of the immunlabeled IMP clusters with the synaptic junction sizes reported by Nyiri et al., (2001) obtained from serial EM section reconstruction of Lowicryl embedded and postembedding immunogold labeled material (single synapse data kindly provided by Dr. G. Nyiri). Summing the immunolabeled IMP cluster areas from samples obtained with the different antibodies gave an average area of 0.0436 ± 0.0273 μm^2 (mean ± SD, n = 183) for somatic and 0.0119 ± 0.0074 μm^2 (n = 13) for axon initial segment synapses. The data published by Nyiri et al., (2001) gave an average somatic synapse area of 0.0812 ± 0.0431 μm^2 (n = 145) and an average synaptic area for the AIS of 0.0357 ± 0.0143 μm^2 (n = 81), both significantly higher (Man Whitney U test, $p< 0.05$) than the values obtained in replica labeling. There can be many reasons for this discrepancy which will be discussed later.

Nevertheless, in view of the high concentration of $GABA_A$ receptors in the synaptic junction, but not outside it, demonstrated with the postembedding method on thin sections (Nusser et al., 1996; Nyiri et al., 2001), the lack of clustered immunolabeling in freeze fracture replica outside the high-density IMP cluster areas leaves no other explanation than the IMP clusters in the P-face being the GABAergic synaptic junctions. This identification of GABAergic synapses will be applied for the subunits $\alpha 1$, $\alpha 2$ and $\beta 3$ of the $GABA_A$ receptor (Fig.4).

On the P-face of replicas, IMPs indicated not only $GABA_A$ receptors, but also many other proteins embedded in the cell membrane (Fujimoto, 1997). To assess the receptor

labeling in the synapses and in the extrasynaptic membrane we delineated labeled synapses on the following joint criteria: 1) more than 5 IMPs in the measured area separated by no more than 30 nm from each other; and; 2) the area was labeled with 2 or more gold particles. This area was defined as the "labeled synaptic area", and the rest of the P-face of that structure was defined as the "extrasynaptic area". In accordance with these criteria, the gold particles on the "synaptic area" indicated "synaptic $GABA_A$ receptor subunits", and the particles on "extrasynaptic area" were associated with "extrasynaptic $GABA_A$ receptor subunits". Sometimes, a piece of pre-synaptic terminal covered part of the post-synaptic membrane; those synapses were not included into the sample of synaptic area measurements, but they were measured and included into the labeling density data.

Freeze-fracture immunolabeling for α1 KO and α2 KO mouse

Replicas prepared from gene knock out (KO) animals were reacted together with replicas from wild type mouse and rats to ensure quality checks for the reactions and reagents (Fig.5). Synapses were recognized by co-labeling with antibodies to the β3 subunit and/or the characteristic P-face IMP clusters (Fig.5A and 5B). There was no synaptic labeling for the α1 or α2 subunits in α1 and α2 KO mice, respectively, but there was labeling for β3 subunit in both mice (Fig.5C and 5D) and for α2 subunit in α1 KO and for α1 subunit in α2 KO mice (Fig.5E and 5F), demonstrating the specificity of our antibodies to the two alpha subunits. This conclusion applies to both the rabbit and rat antibodies to the α1 subunit. One reaction is illustrated in Fig.5A showing α1 and β3 labeling on the cell body of CA1 pyramidal cells in replica of a wild type mouse, and Fig.5C showing double labeling for the same subunits in an α1 KO mouse. Small gold particles (5 nm) indicate α1 labeling and large gold particles (10 nm) indicate β3 subunit labeling. The β3 labeling is concentrated on IMP-clusters demonstrating synaptic labeling on both samples. For the α1 subunit, labeling accumulates on IMP-clusters of wild type synapses, but not in synapses from the α1 KO mouse.

The antiserum to the β3 subunit raised in guinea pig was tested on replicas of β3 KO mouse along with littermate wild type mouse. Reduced synaptic labeling was present over the synaptic IMP clusters in the β3 KO mouse. This shows that the antiserum recognizes proteins other than the β3 subunit that are enriched in the synapses. This is most likely the β2 or β1 subunits because of the sequence homology in the intracellular loop of the protein to which the antiserum was raised. This conclusion is however, in apparent contradiction with the result of the immunofluorescence specificity test using the expression of the β1, β2 and β3 subunits in HEK cells, which showed that only the β3 subunit was recognized (Table A). Therefore, in this thesis I use the term β3 for the immunoreactivity obtained with the guinea pig antibodies raised to the intracellular loop of the β3 subunit. One explanation of the difference in the results is in the replica additional epitopes may be exposed that were not detected under the fluorescence conditions using more strongly fixed sections. These animals tested for the α1 subunit with antibodies raised in rat showed equal labeling over synaptic IMP clusters.

Measuring synaptic area in SDS-FRL and serial ultra-thin sections

On the somata, the synaptic areas obtained were 0.051 ± 0.022 μm^2 (mean ± SD, n=54) μm^2 in the sample for the β3 subunit measurements, 0.053 ± 0.038 μm^2 (n=61) μm^2 for the α1 and 0.041 ± 0.022 μm^2 (n=70) μm^2 for the α2 subunit measurements (Fig.6 and Table B). The sizes of labeled synapses in the tree samples were not significantly different (Kruskal-Wallis ANOVA test, $p > 0.05$), indicating a consistent delineation of synaptic areas. The synaptic area sizes were not normally distributed in any of the the samples in three subcellular compartments (Shapiro-Wilk test, $p < 0.05$), but they were skewed towards larger values (Fig.8B, 10B, 12B and 17).

In order to assess the synaptic area measured in replicas, I also made a measurement in ultra-thin sections from serial sections of conventional epoxy resin-embedded tissue following uranyl acetate and lead citrate contrasting. The length of the synaptic junction

was measured in each section and multiplied by the section thickness. Synaptic junctions were defined as electron opaque cleft material, slight widening of extracellular space, slight postsynaptic thickening and presynaptic vesicle accumulation. The thickness of the sections was 80 μm as read from the ultramicrotome display and confirmed by atomic force microscopy VN-8000 (KEYENCE, Osaka, Japan). The average synaptic area is 0.0800 ± 0.0430 μm^2 (mean ± SD, n=12) for somatic synapses. There are only GABAergic synapses on soma of pyramidal cells, therefore this value can be compared with the value obtained in the replicas. The mean area obtained from the serial ultrathin sections is larger than the mean area obtained from SDS-FRL (Mann-Whitney's U-test, $p < 0.05$).

Density of β3 subunit labeling in distinct subcellular compartments of pyramidal cells

Immunolabeling on the somata, apical dendrites and AISs were compared (Fig.7A-D, and Table B). Double-labeling for the β3 and Nav1.6 subunits enabled the measurements on the AISs. Relationship between synaptic area and β3 labeling was linear on the soma and apical dendrites of CA1 pyramidal cells (Fig.8A), indicating a uniform receptor distribution. The two subcellular compartments did not differ from each other. The number of complete synapses that I could sample on AISs was small (n=4), which excluded their statistical comparison with the other two compartments. Nevertheless, these 4 synapses had a relatively low labeling, but still within the lower end of somatic and dendritic labeling range (Fig.8A). The synaptic labeling densities were skewed towards larger values (Shapiro-Wilk test, $p < 0.05$) (Fig.8C). The densities of labeling for the β3 subunits in synaptic and extrasynaptic areas were not different in the three compartments (Fig.8D). The labeling density in the synaptic areas of the soma was about 100 times higher than in the extrasynaptic areas (Table B).

Density of α1 subunit labeling in distinct subcellular compartments of pyramidal cells

The distribution of labeling using the rat antibodies appeared similar and same

comparisons were attempted as for the β3 subunits (Fig.9A-D). Unfortunately, I could not find fractured complete synapses on Nav1.6 labeled AISs, therefore only the extrasynaptic α1 subunit density could be measured for this compartment (Fig.9C, 9D). There was a strong correlation between the α1 subunit labeling and synaptic area in the somatic and dendritic membranes (Fig.10A). The labeling density in synaptic areas of the soma and apical dendrites was not significantly different and about 100 times larger than in the extrasynaptic membrane (Fig.10C and 10D). The labeling of the extrasynaptic membrane was not different on the soma, apical dendrite and AIS (Table B).

Density of α2 subunit labeling in distinct subcellular compartments of pyramidal cells

The α2 subunit was localized with a purified polyclonal rabbit antibody (Fig. 11A-D). In double labeling of the α2 and Nav1.6 subunits three full and 6 partial synapses were found on AISs (Fig.11C). In this case, a mouse monoclonal anti-Nav1.6 antibody was used as an AIS marker. Overall, the relationship between synaptic area and α2 labeling was strongly correlated in each subcellular compartment (Fig.12A), but there were notable outliers in the somatic and dendritic domains. The densities for α2 in the somatic, apical dendritic and AIS synapse did not differ significantly from each other (Fig.12C and 12D). Like with the other antibodies the labeling density of the synaptic areas on the soma was about 100 times higher than that of the extrasynaptic membrane (Table B).

Comparison of synapse size and synaptic/extrasynaptic labeling ratio on three domains of pyramidal cells

Overall, the different antibodies to the three subunits (α1, α2 and β3) produced very similar results (Fig.13A, and Table.B).

The synaptic areas on the somata (Kruskal-Wallis ANOVA test, $p > 0.05$) and dendrites were similar from the three measurements with one exception. The sample of dendritic synapses obtained from the replica reacted for the α2 subunit has a significantly

smaller size from the other two samples as seen most clearly in the cumulative probability plot in (Fig.13C) and was also shown by a statistical test (Kruskal-Wallis ANOVA with posthoc Dun test, $p< 0.05$). However, the synapses on the AIS were smaller than in the other two compartments, confirming the results of Nyiri et al., (2001) obtained from serial reconstructions from thin sections. It appears that the synaptic areas in each subcellular compartment were not different for the four different $GABA_A$ subunits and this indicates that they may label the same synapse population.

The ratio of synaptic labeling density to extrasynaptic labeling density in distinct subcellular compartments of the CA1 pyramidal cells was also compared (Fig.13D, Table C). The affinities of the antibodies differ from each other, therefore it is not meaningful to compare labeling densities between antibodies. However it is noteworthy that the ratios of synaptic to extrasynaptic labeling densities were almost the same for α1 and α2 subunits in both the soma and the apical dendrite.

The somatic and apical dendritic labeling ratios did not differ for all subunits. The ratio for the β3 subunits on AISs was lower than that on somata and dendrites, but the low number of AISs found precluded further analysis. Similarly, the number of synaptic areas that I could measure on AISs in the samples for the α2 (n=6) and β3 (n=3) subunits were small.

Co-localization of β3 and α1 or α2 subunit

In the hippocampus, the β3 subunit of the $GABA_A$ receptor is the major β subunit and because the β subunit is an obligatory member of the receptor it is expected that most GABAergic synapses on pyramidal cells would contain the β3 subunit. We examined what proportion of β3 subunit labeled synapses on the soma contain either the α1 or the α2 subunit, because previous studies indicated that these two subunits may be segregated in somatic synapses (Nyiri et al., 2001, Klausberger et al., 2002, Thomson et al., 2000).

The reaction of antibodies was carried out sequentially, so the antibody to the α

subunit was applied first followed by secondary antibody with colloidal 5 nm gold particles. Then the primary antibody to the β3 subunit was applied, and finally secondary antibody with 10 nm gold particles was added. Only synapses labeled for the β3 subunits (10 nm gold) were measured in these experiments. I chose such a sequential reaction in order to avoid decreasing the amount of antibody to the α subunit by potential sterical hindrance by antibodies to the β3 subunit. There is a possibility that some GABAergic synapses were not labeled for the β3 subunits for two reasons. First, some synapses may not include β3 subunits. A second, technical reason for negative result might arise because of sterical hindrance by the first layer of antibodies preventing either the second primary antibody or the second layer of gold conjugated antibodies from binding to the replica, and thus producing false negative results. To test for false negative reactions, antibodies in inverse order were also applied. Following double-labeling experiments, only the somatic population of synapses were analysed, because of the demanding nature of the data collection.

In replicas labeled with α1 antibody and β3 antibody, 81% of β3 positive synapses (10 nm gold particles) were also labeled with antibodies to the α1 subunit (5 nm gold). In the inverse order reaction, 96% of the α1 positive synapses were also positive for the β3 subunits (Fig.14, Table D). These results indicated that α1 positive synapses always contain β3 subunits, and that about 80% of β3 positive synapses contain α1 subunits in the same synapse.

Sequential double-labeling with antibodies to the α2 and β3 subunits showed a high frequency of double-positive synapses on somata. Interestingly, labeling for the α2 and β3 subunits gave similar results to the α1 labeling (Fig.15, Table C). Of all the β3 positive synapses 83% were labeled for the α2 subunit, and all α2 positive synapse contained labeling for the β3 subunits (Table C). As mentioned above, labeling for the β3 subunits were used to identify GABAergic synapses. If labeling for the β3 subunits could detect all GABAergic synapses on soma of CA1 pyramidal cells, a high proportion of GABAergic

synapses would include both the α1 and α2 subunits. To examine this prediction directly, double labeling with antibodies to the α1 and α2 subunits was carried out.

Co-localization of the α1 and α2 subunits

Double labeling with antibodies to the α1 subunits and α2 subunits resulted in a high frequency of double labeled synapses (Fig.16). In the labeling using antibodies to the α1 subunit first (5 nm particles) followed by antibodies to the α2 subunit (10 nm particles), most of the synapses labeled for the α2 subunit were double labeled (97%, Table C). Similarly, in the reverse order reaction, most α1 subunit labeled synapses also contained labeling for the α2 subunit (87%, Table C). These results suggest that the α1 subunit is co-localized with the α2 subunit in most, if not all, synapses that include one of these subunits on the soma of hippocampal CA1 pyramidal cells.

Fig.17 shows the distributions of synaptic areas in single and double labeling. To test if the synapses populations in single labeling are same to those in double labeling, these distributions were compared. I found no significant difference in size of synaptic areas between double labelings (Fig.17A-C). However synaptic areas in single labelings were smaller than those in double labelings (Kruskal-Wallis ANOVA test, $p < 0.05$). This result probably reflects higher sensitivity in single labeling, which detected small synapses that were not labeled with 10 nm gold particles used for double labelings.

It does not indicate that I observed different synapses in single and double labeling. In single labelings, synapses are labeled with 5 nm gold particles, and 10 nm gold particles are marker for synapses in double labelings. Small particles can detect easily small synapses, so synaptic are in single labelings are skewed towards smaller values.

The double labeling experiments with α1, α2 and β3 subunit specific antibodies indicated that: 1) 80% of β3 positive GABAergic synapses on soma include α1 or α2 subunits, and 2) α1 subunits and α2 subunits are almost always co-localized in the same

synapses. These results lead to the conclusion that of the GABAergic synapses that are labeled for the β3 subunits, about 20% may not be labeled for either the α1, or the α2 subunits. If our labeling efficacy is high, the synapses immunonegative for both the α1 and α2 subunits could form a distinct functional population in which synaptic signaling is mediated by other types of $GABA_A$ receptors, for example, $GABA_A$ α5 subunit.

5. DISCUSSION

Definition of synapses in freeze fracture replica

In thin, electron microscopic sections, one criterion for a synaptic junction is the clustering of synaptic vesicles at the presynaptic membrane at the active zone. This criterion is not available in freeze fracture replicas. We noticed that the P-face replica of the soma of pyramidal cells contained small island of high density IMPs that resembled in size and frequency the synapses that these cells receive from the GABAergic basket cells. In these islands the IMPs are more loosely arranged and the distance between them is more variable than in gap junctions (Dudek et al., 1998; Rash et al., 2001) that have a characteristic arrangement in freeze fracture replicas. To my knowledge, such IMP islands have not been described earlier in the somatic P-face. Similar IMP islands have been demonstrated in the E-face of replicated glutamatergic synapses corresponding to high density AMPA type glutamate receptor labeling (Tanaka et al., 2005; Fukazawa et al., 2004 Soc Neurosci). In facing replicas of the E- and P-faces of glutamatergic synapses, no IMPs were apparent in the P-face in the synaptic area where the E-face contained high density IMP clusters. I did not attempt to produce facing replicas of the same synapses of CA1 pyramidal cells, but in E-face replicas of the plasma membrane islands of IMPs with similar size to P-face islands of GABAergic synapses were not found. Therefore, I conclude that GABAergic synapses on pyramidal cells result in IMP clusters in the P-face, in contrast to glutamatergic synapses which result in IMP clusters in the E-face.

Indeed, as expected, immunolabeling with antibodies to $GABA_A$ receptor subunits showed a high density of immunogold particles over these islands, suggesting that they were basket cell synapses. This assumption is supported by previously published immunogold results using the postembedding technique on several neuronal types, including CA1 pyramidal cells, which showed that the synaptic junction, as defined in electron micrographs, contains a high density of $GABA_A$ receptors (Nusser et al., 1996;

Somogyi et al., 1996; Klausberger et al., 2002). Although extrasynapic $GABA_A$ receptor immunoreactivity has been also demonstrated by immunogold techniques, the latter did not show high concentration islands similar to the synaptic junctions (Nusser et al., 1996; Nyiri et al., 2001).

To explore further the correspondence of high density IMP clusters and electron microscopically reconstructed synaptic junctions from thin sections, I compared the sizes of these two populations, basing serially reconstructed areas from thin section published by Nyiri et al., (2001) on somatic and AIS synapses on CA1 pyramidal cells. The IMP islands having $GABA_A$ receptor subunit labeling were significantly smaller on both the soma and the AIS as compared to serial reconstruction data. There can be several explanations for this discrepancy that can only be clarified with further experiments. First, the thin section data of Nyiri et al., (2001) derives from Lowicryl embedded material that has low contrast due to the lack of osmium in the tissue. Therefore, the definition of the edges of the synaptic junctions may be difficult to achieve and this could lead to overestimation of the length of the membrane specialization in single section. Furthermore, it is possible that puncta adherentia, which are frequently adjacent to GABAergic synapses, but do not contain receptors, were included in the measurement of synaptic junctions. Secondly, Nyiri et al., (2001) estimated section thickness from microtome setting (personal communication), which may have resulted in an overestimation of section thickness and consequently the synaptic junctional area. On the other hand, the delineation of IMP clusters may have also resulted in an underestimation of synaptic junctions. Because replica immunolabeling is a highly sensitive method, it shows abundant extrasynaptic receptors, some of which are associated with small IMP clusters that may not be synapses. My criterion for synapses as 5 or more IMPs and at least two gold particles, possibly included some small non-synaptic clusters that led to an underestimation of synaptic areas. Unfortunately, there is no known abundant GABAergic synaptic scaffolding protein, like PSD-95 for glutamatergic synapses, that could be used for delineating synaptic junctions

with an independent molecular marker. We have attempted to use antibodies to gephyrin, but obtained no labeling in SDS-FRL. Although it is disappointing that the $GABA_A$ receptor labeled IMP cluster size does not match the published GABAergic synaptic area obtained from thin sections, at present the most parsimonious explanation for the high density IMP clusters labeled by antibodies to $GABA_A$ receptors is that they represent synaptic junctions. Clearly a more accurate thin section synaptic area measurement is needed from epoxy resin embedded optimally fixed material for comparison of sizes.

Nav1.6 as a marker for AISs

The AIS is thought to be the site of action potential generation and it has unique fine structural characteristics, such as the electron dense membrane undercoating and fasciculated microtubules (Kosaka, 1980). In several neuronal types it has also been shown to be highly enriched in voltage gated sodium channels as shown by immunocytochemistry (Gong et al., 1999; Trimmer and Rhodes, 2004). Voltage gated sodium channels consist of α and β subunits the α subunit giving the channels distinct functional properties and the expression of α subunits is highly cell type specific. Hippocampal pyramidal cell express several α subunits and in particular the Nav1.6 subunit at high level. Indeed this subunit has been demonstrated in the AIS in cultured pyramidal cells, therefore I tested if it could be used as a molecular marker for the AIS in situ in the brain. The light microscopic results strongly suggested that the AISs of pyramidal cells are labeled. In immunlabeled replicas I found that the P-face of radially oriented cylindrical structures with the expected size of AIS were immunolabeled in an apparently diffuse manner. Such structures were very rare and the sample of 14 AISs collected in this study took several weeks of electron microscopic time to obtain. Unexpectedly, IMP clusters representing GABAergic synapses most likely made by the so-called axo-axonic cells were very rare and small in area. About half of these synapses were not complete, because either part of the presynaptic terminal or neighboring cellular processes covered some of the IMP cluster. Thus, it is possible that on

the AIS, due to its transmembrane protein composition, the fracture plane does not readily travels through the GABAergic postsynaptic membrane and it is even possible that the sample was therefore biased towards smaller synaptic junctions.

Technical considerations of freeze fracture replica immunolabeling

Freeze fracture immunolabelig is a highly sensitive technique that provides high-resolution two dimensional quantitative maps of proteins in cell membranes (Rash et al., 2001; Tanaka et al., 2005; Hagiwara et al., 2005). The sensitivity of the techniques is well documented by the quantitative comparison of receptor immunolabeling with functional receptor numbers in glutamatergic synapses, where Tanaka et al., (2005) demonstrated that one 5 nm immunogold particle roughly corresponded to one functional synaptic AMPA receptor channel. Postembedding immunogold labeling of synaptic receptors is also possible in thin sections of acrylic resin embedded tissue and there are numerous reports on different cell types and receptors in the brain. However, even in acrylic resin, most of the tissue within the electron microscopic section is not accessible to antibodies, which only recognize epitopes on the surface of sections. The preembedding method is not suitable for detecting synaptic receptors, because the antibodies have no access to the epitopes in the dense protein matrix in fixed tissue without proteinase treatment.

In this study, I measured the labeling density of $GABA_A$ receptor subunits in distinct subcellular compartments. The distribution of some of these subunits have been reported previously by conventional post-embedding methods and the labeling density of $GABA_A$ receptors have been estimated in several cell types (Nusser, et al., 1995; Nusser, et al., 1996). The improvement provided by SDS-FRL is the possibility of observing cell membranes in two-dimensional manner and the better quantification resulting from the high sensitivity. In thin section electron microscopy, the plasma membrane of the synaptic junction is recognized as a line or as a band in tangential sections, but the freeze fractured

cell membrane appears as a sheet. Reconstruction of synapses from serial sections is hampered by the partially tangential section plane in the post-embedding method, but SDS-FRL method can show the whole synaptic disc in one image in spite of undulations in the membrane. The other advantage of the SDS-FRL method is the removal of membrane associated proteins which are anchored to but not integrated in the cell membrane and may mask epitopes on the receptor proteins. The membrane integrated proteins, such as receptors, are exposed on the replica by the SDS digestion and this makes easy access to them by the antibodies.

But there are also some limitations of the SDS-FRL method. The major problem is a lack of morphological clues to identify the membranes of cells and processes under study. The most obvious missing information in the context of the present study is the absence of the presynaptic terminal at the sites of synaptic junctions. In the hippocampal CA1 area the recognition of the pyramidal cells is not a problem due to their high abundance and strict laminar location. However, the recognition of GABAergic interneurons and their dendrites is much more difficult due to their lower abundance and less regular organization in the tissue.

Subunit composition of GABAergic synapse populations on CA1 pyramidal cells

Usually a single $GABA_A$ receptor has 2 α subunits. The results suggest that there are α1 and α2 $GABA_A$ receptor subunits in some single synapses, however, we cannot establish if several α subunit species are in a single receptor channel or each α subunit is present only in a channel that contains only that subunit.

In the present study I showed that about 80% of β3 positive synapses include both the α1 and α2 subunits. My results appear to contradict the conclusions of previous reports (Nyiri, 2001, Klausberger, 2002). Based on postembedding immunolabelling, they reported two kinds of GABAergic synapses on the soma of pyramidal cells made by presynaptic terminals positive for parvalbumin, a molecular marker for one type of basket cell

(Katsumaru et al., 1988), or negative for parvalbumin. They suggested that the latter synapses were made by cholcystokinin positive basket cells. Synapses made by parvalbumin positive terminals were more immunoreactive for the α1 subunit, whereas synapses made by parvalbumin negative boutons were more immunopositive for the α2 subunit. These conclusions were drawn from different experiments using antibodies to one subunit only. Paired in vitro recording of single GABAergic cell responses in pyramidal cells seemed to support these conclusions (Thomson et al., 2000).

One of the advantages in SDS-FRL is higher sensitivity than the postembedding method and the detection of two distinct α subunits in the same synapses. The co-existence of α1 and α2 subunits in a large proportion of synapses on the soma shows that these subunits are not segregated, but might instead be in different proportions in synapses established by parvalbumin or cholecystokinin expressing basket cells. In my experiments, I have not been able to correlate the amount of α1 and α2 subunit immunoreactivity in single synapses. One reason for this is the lower labeling efficacy of the 10 nm gold particle coupled secondary antibody due to sterical hindrance. To measure the relative amount of two receptor subunits it will be necessary to develop normalization procedures with ranges of antibody dilutions to balance the two signals in simultaneous rather than sequential applications of two antibodies. In conclusion, my results and the previous postembedding results may not necessarily be contradictory, if there were a reverse correlation of α1 or α2 subunit containing receptors in synapses innervated by the two distinct basket cells and future quantitative SDS-FRL studies can confirm this.

The final question is which subunit is expressed in the 20% of β3 positive synapses that are immunonegative for the α1 or α2 subunits . Pyramidal cells in CA1 area expressed particularly α1, α2 and α5 subunit, so α5 subunit is the most reasonable candidate. However it is not clear whether somatic synapses containing the α5 subunit which has the unique pharmacological property of having extremely low affinity for zolpidem, a type 1 benzodiazepine agonist, are distinct or overlapping with the α1 and α2

subunit containing synapse populations.

Co-assembly of α subunits in a single $GABA_A$ channel

According to the conventional classification scheme, $GABA_A$ receptors are divided into 3 types (Johnston, 2005). This classification depends on the pharmacology of the benzodiazepine binding site. Many neurons express more than three different subunits of the pentameric $GABA_A$ receptors, which mostly consist of two α two β and one γ subunits, but the γ subunit might be replaced by δ or ε or π subunits and the β subunit might be replaced by τ subunit. In addition there are three β, six α and 3 ρ subunits, giving a total of 19 genes. Pyramidal cells in the CA1 area express at least 14 subunits (Wisden et al., 1992; Sperk et al., 1997) as indicated by in situ hybridizaiton and immunohistochemical studies (Wisden et al., 1992; Sperk et al., 1997; Ogurusu et al., 1999; Pirker et al., 2000), but the precise subunit composition of not a single receptor type is known biochemically. Using subunit specific pharmacological tools it has been predicted that many receptors include α1βγ2 subunits and probably separately α2βγ2 subunits and in addition α5βγ2 subunits. However, it has been demonstrated in cerebellar granule cells that the same receptor channel may include more than one α subunit species and/or more than one β subunit species, making the receptor pharmacology difficult to predict (Jechlinger et al., 1998). For example, at least some immunoaffinity purified α5 subunit containing receptors in the hippocampus include the α1 subunit, but nevertheless exhibit an α5 subunit specific pharmacological profile (Araujo et al., 1999). In addition to the α subunit, the identity of γ subunit also contributes to the benzodiazepine pharmacology of the $GABA_A$ receptor complex, because the benzodiazepine binding site of the $GABA_A$ receptor complex is formed by the interface between α and γ subunits (Sigel and Buhr, 1997).

Synaptic receptors are thought to include the γ2 subunit, which interacts with the postsynaptic protein matrix and is thought to be necessary for receptor anchoring. When the γ2 subunit is replaced by the δ subunit, as in cerebellar granule cells the receptors are

only located outside the synaptic specialization. In this respect, it would be interesting to know which subunits are associated with the δ subunit in CA1 pyramidal cells, which would provide a clue to the subunit composition of at least one receptor population. More importantly, the question arises whether these represent distinct receptor populations, or at least two distinct α subunits in one receptor channel. This question cannot be answered at present unequivocally. Unfortunately, the immunogold labeling method does not have the resolution to resolve different subunits in a single receptor. Furthermore, receptor extraction for subunit content analysis looses site and cell type information. For example, many studies concluded from rat whole brain that two homologous or different α subunits are co-assembled in a single $GABA_A$ receptor (Duggan et al., 1991; Pollard et al., 1993; Mertens et al., 1993), but they did not distinguish synaptic receptors from extrasynaptic receptors, or different cell types of origin. As discussed above, the receptor pharmacology of synaptic responses obtained by stimulating single presynaptic GABAergic neurons in paired in vitro recordings suggest that at least some synapses are dominated by a particular α subunit receptor pharmacology. Whether this represents receptors containing only one α subunit species or at least some receptors contain two species, but nevertheless the response is dominated by one α subunit remains to be investigated.

Synaptic versus extrasynaptic $GABA_A$ receptors

Immunoparticle density for all subunits investigated showed a higher concentration over high density IMP clusters, the synapses, than over the extrasynaptic plasma membrane. This was particularly surprising for the α5 subunit, which has been suggested to be exclusively or mainly extrasynaptic (Caraiscos et al., 2004; Crestani et al., 2002; Fritschy and Bruning, 2003). However, at least one previous immunhistochemical publication has reported that the α5 subunit is concentrated in GABAergic synapses of cultured hippocampal pyramidal cells (Christie and Blas, 2002).

The synaptic junctions on the soma probably cover less than 1% of the cell surface.

In view of the 80-100 times concentration of labeling over synapses and assuming 0.8-1% synaptic coverage of the soma, it can be estimated that the absolute amount of labeling is about the same in the synapses and in the extrasynapic membrane. Assuming a linear relationship between labeling and receptor number, the number of receptors in synapses and in the extrasynaptic memberane may be similar even on the soma that has the highest density of GABAergic synapses. The density of GABAergic synapses decreases on the apical dendrite and probably even more on the thin oblique dendritic branches which together with the dendritic spines constitute most of the pyramidal cell surface. The dendritic spines of pyramidal cells in the CA1 receive little GABAergic innervation (Megias et al., 2001). The total amount of extrasynaptic receptor on the neuronal surface may be several fold higher than the synaptic receptor for the tested subunits, because of the declining density of GABAergic synapses away from the soma.

The above prediction assumes that the immunogold labeling density is linearly related to receptor density. This might not always be the case. I was careful to chose primary antibody concentrations that do not result in a saturation of the signal over the synaptic junctions, i. e. in all cases using more concentrated primary antibody than the one applied in the quantitative measurements, increased the synaptic labeling density. Because the synapses contain a high density of receptors, the antibodies may not have access to all the eptitopes resulting in an under-estimation of synaptic receptor density. The second antibody that was conjugated to the gold particles may also have sterical hindrance over the synapses, which is indicated by the fact that over synapses using 5 nm gold particles results in roughly twice the gold density compared to 10 nm gold particles.

6. LITERATURE CITED

Anderson P, Bliss T V and Skrede K K (1971) Lamellar organization of hippocampal pathways. Exp Brain Res 13:222-238.

Araujo F, Tan S, Ruano D, Schoemaker H, Benavides J and Vitorica J (1996) Molecular and pharmacological characterization of native cortical gamma-aminobutyric acid (A) receptors containing both α(1) and α(3) subunits. J Biol Chem 271:27902-27911.

Araujo F, Ruano D and Vitorica J (1999) Native gamma-aminobutyric acid type A receptors from rat hippocampus, containing both alpha 1 and alpha 5 subunits, exhibit a single benzodiazepine binding site with alpha 5 pharmacological properties. J Pharmacol Exp Ther 290:989-997.

Baumann S W, Baur R and Sigel E (2001) Subunit arrangement of γ-aminobutyric acid type A receptors. J Biol Chem 276:36275-36280.

Baumann S W, Baur R, and Sigel E (2002) Forced subunit assembly in α1β2γ2 $GABA_A$ receptors. Insight into the absolute arrangement. J Biol Chem 277:46020-46025.

Benke D, Honer M, Michel C and Mohler H (1996) GABA(A) receptor subtypes differentiated by their gamma-subunit variants: Prevalence, pharmacology and subunit architecture. Neuropharmacology 35:1413-1423.

Benavides J, Peny B, Ruano D, Vitorica J and Scatton B (1993) Comparative autoradiographic distribution of central omega (benzodiazepine) modulatory site subtypes with high, intermediate and low affinity for zolpidem and alpidem. Brain Res 604:240-250.

Bragin A, Jando G, Nadasdy Z, Hetke J, Wise K and Buzsaki G (1995) Gamma (40-100 Hz) oscillation in the hippocampus of the behaving rat. J Neurosci 15:47-60.

Brunig I, Scotti E, Sidler C and Fritschy J M (2002) Intact sorting, targeting, and clustering

of γ-aminobutyric acid A receptor subtypes in hippocampal neurons in vitro. J Comp Neurol. 443:43-55.

Buhl E H, Halasy K and Somogyi P (1994) Diverse sources of hippocampal unitary inhibitory postsynaptic potentials and the number of synaptic release sites. Nature 198:823-828.

Caraiscos V B, Elliott E M, You-Ten K E, Cheng V Y, Belelli D, Newell J G, Jackson M F, Lambert J J, Rosahl T W, Wafford K A, MacDonald J F and Orser B A (2004) Tonic inhibition in mouse hippocampal CA1 pyramidal neurons is mediated by α5 subunit-containing γ-aminobutyric acid type A receptors. Proc Natl Acad Sci USA 101: 3662-3667;

Chang Y, Wang R, Barot S and Weiss D S (1996) Stoichiometry of a recombinant $GABA_A$ receptor. J Neurosci 16:5415-5424.

Cherubini E and Conti F (2001) Generating diversity at GABAergic synapses. Trends Neurosci 24:155-162.

Christie S B and Blas A L (2002) α5 subunit-containing $GABA_A$ receptors form clusters at GABAergic synapses in hippocampal cultures. Neuroreport 13:2355-2358.

Cobb S R, Buhl E H, Halasy K, Paulsen O and Somogyi P (1995) Synchronization of neuronal activity in hippocampus by individual GABAergic interneurons. Nature 378: 75-78.

Crestani F, Keist R, Fritschy J M, Benke D, Vogt K, Prut L, Bluthmann H, Mohler H and Rudolph U (2002) Trace fear conditioning involves hippocampal α5 $GABA_A$ receptors. Proc Natl Acad Sci USA 99:8980-8985.

Csicsvari J, Hirase H, Czurko A, Mamiya A and Buzsaki G (1999) Oscillatory coupling of hippocampal pyramidal cells and interneurons in the behaving rat. J Neurosci 19:274-287.

Davies P A, Hanna M C, Hales T G and Kirkness E F (1997) Insensitivity to anaesthetic agents conferred by a class of $GABA_A$ receptor subunit. Nature 385:820-823.

Dudek F E, Yasumura T and Rash J E (1998) 'Non-synaptic' mechanisms in seizures and epileptogenesis. Cell Biol Int 22:793-805.

Duggan MJ, Pollard S and Stephenson FA (1991) Immunoaffinity purification of $GABA_A$ receptor a-subunit iso-olidomers. J Biol Chem. 266:24778-24784.

Donna M Krzemien, Kristin L. Schaller, S. Rock Levinson and John H. Caldwell (2000) Immunolocalization of sodium channel isoform NaCh6 in the Nervous system. J Comp Neuro 420:70-83.

Fisahn A, Pike F G, Buhl E H and Paulsen O (1998) Cholinergic induction of networks oscillations at 40Hz in the hippocampus in vitro. Nature 394: 186-189.

Freund T F and Buzsaki G (1996) Interneurons of the hippocampus. Hippocampus 6: 347-470.

Fritschy J M, Weinmann O, Wenzel A and Benke D (1998) Synapse-specific localization of NMDA and GABAA receptor subunitsrevealed by antigen retrieval immunohistochemistry. J Comp Neurol 390:194-210.

Fritschy J M and Brunig I (2003) Formation and plasticity of GABAergic synapses: physiological mechanisms and pathophysiological implications. Pharmacol Ther 98:299-323.

Fujimoto K (1995) Freeze-fracture replica electron microscopy combined with SDS digestion for cytochemical labeling of integral membrane proteins. Application to the immunogold labeling of intercellular junctional complexes. J Cell Sci 108:3443-3449.

Fujimoto K (1997) SDS-digested freeze-fracture replicallabeling electron microscopy to study the two-dimensional distribution of integral membrane proteins and phospholipids in biomembranes: practical procedure, interpretation and application. Histochem Cell Biol 107:87-96.

Fukuda T and Kosaka T (2000) The dual network of GABAergic interneurons linked by both chemical and electrical synapses: a possible infrastructure of the cerebral

cortex. Neurosci Res. 38:123-30.

Gong B, Rhodes K J, Bekele-Arcuri Z and Trimmer J S (1999) Type I and type II Na(+) channel alpha-subunit polypeptides exhibit distinct spatial and temporal patterning, and association with auxiliary subunits in rat brain. J Comp Neurol. 412:342-52.

Gulyas A I, Miles R, Hajos N and Freund T F (1993) Eur J Neurosci 5:1729-1751.

Hagiwara A, Fukazawa Y, Deguchi-Tawarada M, Ohtsuka T and Shigemoto R (2005) Differential distribution of release-related proteins in the hippocampal CA3 area as revealed by freeze-fracture replica labeling. J Comp Neurol 2005:195-216.

Hall C E (1950) A low temperature replica method for electron microscopy. J Appl Phys 21:61-67.

Hedblom E and Kirkness E F (1997) A novel class of $GABA_A$ receptor subunits in tissues of the reproductive system. J Biol Chem 272:15346-15350.

Hevers W and Luddens H (1998) The diversity of $GABA_A$ receptors. Pharmacological and electrophysiological properties of $GABA_A$ channel subtypes. Mol Neurobiol 18:35-86.

Horenstein J, Wagner D A, Czajkowski C and Akabas M H (2001) Protein mobility and GABA-induced conformational changes in $GABA_A$ receptor pore-lining M2 segment. Nature Neurosci 4:477-485.

Houser C R and Esclapez M (2003) Downregulation of the alpha5 subunit of the GABA(A) receptor in the pilocarpine model of temporal lobe epilepsy. Hippocampus 13:633-645.

Jechlinger M, Pelz R, Tretter V, Klausberger T and Sieghart W (1998) Subunit composition and quantitative importance of hetero-oligomeric receptors: $GABA_A$ receptors containing alpha6 subunits. J Neurosci. 18:2449-2457.

Johnston G A R (1996) $GABA_A$ receprot pharmacology. Pharmacol Therap 69:173-198.

Johnston G A R (2005) $GABA_A$ receprot channel pharmacology. Curr Pharm Des 11:1867-1885.

Katsumaru H, Kosaka T, Heizmann C W and Hama K (1988) Immunocytochemical study of GABAergic neurons containing the calcium-binding protein parvalbumin in the rat hippocampus. Exp Brain Res. 72:347-362.

Klausberger T, Roberts J D B and Somogyi P (2002) Cell type- and input-specific differences in the number and subtypes of synaptic $GABA_A$ receptors in the hippocampus. J Neurosci 22:2513-2521.

Klausberger T, Magill P J, Marton L F, Roberts J D B, Cobden P M, Buzsaki G and Somogyi P (2003) Brain state- and cell type-specific firing of hippocampal interneurons in vivo. Nature 421:844-848.

Kosaka T (1980) The axon initial segment as a synaptic site: ultrastructure and synaptology of the initial segment of the pyramidal cell in the rat hippocampus (CA3 region). J Neurocytol 9:861-882.

Kosaka T, Wu J Y, Benoit R (1988) GABAergic neurons containing somatostatin-like immunoreactivity in the rat hippocampus and dentate gyrus. Exp Brain Res. 71:388-398.

Lacaille J-C and Schwartzkroin P A (1988) J Neurosci 8:1400-1410.

Mann E O, Radcliffe C A and Paulsen O (2005) Hippocampal gamma-frequency oscillations: from interneurones to pyramidal cells, and back. J Physiol 562:55-63.

McBain C J, DiChiara T J and Kauer J A (1994) J Neurosci 14:4433-4445.

Megías M, Emri Zs, Freund F and Gulyás A I (2001) Total number and distribution inhibitory and excitatory synapses on hippocampal CA1 pyramidal cells. Neuroscience 102:527-540.

Mertens S, Benke D and Mohler H, (1993) $GABA_A$ receptor populations with novel subunit combinations and drug binding profiles identified in brain by alpha 5- and delta-subunit-specific immunopurification. J Biol Chem. 1993. 268:5965-73.

Miles R, Toth K, Gulyas A, Hajos N and Freund T F (1996) Differences between somatic and dendritic inhibition in the hippocampus. Neuron. 16:815-823.

Moss S J, and Smart T G (2001) Constructing inhibitory synapses. Nature Rev Neurosci. 2:240-250.

Nayeem N, Green T P, Martin I L and Barnard E A (1994) Quaternary structure of the native $GABA_A$ receptor determined by electron microscopic image analysis. J Neurochem 62:815-818.

Nyiri G, Freund T F and Somogyi P (2001) Input-dependent synaptic targeting of α2-subunit-containing $GABA_A$ receptors in synapses of hippocampal pyramidal cells of the rat. Eur J Neurosci.13:428-442.

Nusser Z, Roberts J D B, Baude A, Richard J G and Somogyi P (1995) Relative densities of synaptic and extrasynaptid GABAA receptors on cerebelar granule cells as determined by a quantitative immunogold method. J Neurosci. 15:2948-2960.

Nusser Z, Sieghart W, Benke D, Fritschy J M and Somogyi P (1996) Differntial synaptic localization of two major γ-aminobutyric acid type A receprtor α subunits on hippocampal pyramidal cells. Proc Natl Acad Sci USA. 93:11939-11944.

Ogurusu T, Yanagi K, Watanabe M, Fukaya M and Shingai R (1999) Localization of GABA receptor rho 2 and rho 3 subunits in rat brain and functional expression of homooligomeric rho 3 receptors and heterooligomeric rho 2 rho 3 receptors. Receptors Channels. 6:463-475.

O'Keefe J and Recce M L (1993) Phase relationship between hippocampal place units and the EEG theta rhythm. Hippocampus. 3:317-330.

Persohn E, Malherbe P and Richards J G (1992) Comparative molecular neuroanatomy of cloned $GABA_A$ receptor subunits in the rat CNS. J Comp Neurol. 326:193-216.

Pirker S, Schwarzer C, Wieselthaler A, Sieghart W and Sperk G (2000) $GABA_A$ receptors:Immunocytochemical distribution of 13 subunits in the adult rat brain. Neuroscience. 101:815-850.

Prichatt D B, Luddens H and Seeburg P H (1989) Type I and type II $GABA_A$-benzodiazepine receptors produced in transfected cells. Science.

245:1389-92.

Pollard S, Duggan M J and Stephenson F A (1993) Further evidence for the existence of α subunit heterogeneity within discrete gamma-aminobutyric $acid_A$ receptor subpopulations. J Biol Chem 268:3753-3757.

Rash J E, Yasumura T, Dudek F E and Nagy J I (2001) Cell-specific expression of connexins and evidence of restricted gap junctional coupling between glial cells and between neurons. J Neurosci. 21:1983-2000.

Ruano D, Vizuete M, Cano J, Machado A and Vitorica J (1992) Heterogeneity in the allosteric interactions between the GABA binding site and three different benzodiazepine binding sites of the $GABA_A$/benxodiazepine receptor complex in the rat nervous system. J Neurochem. 58:485-493.

Schaller K L and Caldwell J H (2000) Developmental and regional expression of sodium channel isoform Nach6 in the rat central nervous system. J Comp Neurol. 20:84-97.

Scollve W B and Milner B (1957) Loss of recent memory after bilateral hippocampal lesions. J Neurol Psycheatry. 20: 11-21.

Sieghart W (1995) Structure and pharmacology of gamma-aminobutyric acid A receptor subtypes. Pharmacol Rev. 47:181-234.

Sieghart W, Fuchs K, Tretter V, Ebert V, Jechlinger M, Hoger H and Adamiker D (1999) Structure and subunit composition of $GABA_A$ receptors. Neurochem Int. 34:379-385.

Sieghart W and Sperk G (2002) Subunit composition, distribution and function of GABA(A) receptor subtypes. Curr Top Med Chem. 2:795-816.

Sigel E and Buhr A (1997) The benzodiazepine binding site of $GABA_A$ receptors. Trends Pharmacol Sci. 18:425-429.

Sik A, Penttonen M, Ylinen A and Buzaki G (1995) Hippocampal CA1 interneurons: an in vivo intracellular labeling study. J Neurosci. 15; 6651-6665.

Skaggs W E, McNaughton B L, Wilson M A and Barnes C A (1996) Theta phase

precession in hippocampal neuronal populations and the compression of temporal sequences. Hippocampus. 6:149-172.

Sperk G, Schwarzer C, Tsunashima K, Fuchs K and Sieghart W (1997) $GABA_A$-receptor subunits in the rat hippocampus-I. Immnocytochemical distribution of thirteen subunits. Neuroscience. 80:987-1000.

Somogyi P, Nunzi M G, Gorio A and Smith A D (1983) A new type of specific interneuron in the monkey hippocampus forming synapses exclusively with the axon initial segments of pyramidal cells. Brain Res. 259:137-142.

Somogyi P, Fritschy J M, Benk D, Roberts J D B and Sieghart W (1996) The γ2 subunit of the $GABA_A$ receptor is concentrated in synaptic junctions containing the α1 and β2/3 subunits in hippocampus, cerebellum and globus pallidus. Neuropharmacology. 35:1425-1444.

Somogyi P, Tama´s G, Lujan R and Buhl E H (1998) Salient features of synaptic organisation in the cerebral cortex. Brain Res Rev. 26:113-135.

Somogyi P and Klausberger T (2005) Defined types of cortical interneurone structure space and spike timing in the hippocampus. J Physiol 562:9-26.

Sur C, Wafford K A, Reynolds D S, Hadingham K L, Bromidge F, Macaulay A, Collinson N, O'Meara G, Howell O, Newman R, Myers J, Atack J R, Dawson G R, McKernan R M, Whiting P J, Rosahl T W (2001) Loss of the major $GABA_A$ receptor subtype in the brain is not lethal in mice. J Neurosci 21:3409-3418.

Takizawa T and Saito T (1996) Freeze-fracture enzyme cytochemictry: application of enzyme cytochemistry to freeze-fracture cytochemistry. J Electron Microsc. 45:242-246.

Tanaka J, Matsuzaki M, Tarusawa E, Momiyama A, Molnar E, Kasai H and Shigemoto R (2005) Number and density of AMPA receptors in single synapses in immature cerebellum. J Neurosci 25:799-807.

Thomson A M, Bannister A P, Hughes D I and Pawelzik H (2000) Differential sensitivity to

Zolpidem of IPSPs activated by morphologically identified CA1 interneurons in slices of rat hippocampus. Eur J Neurosci. 12:425-436.

Torrisi M R and Mancini P (1996) Freeze-fracture immunogold labeling. Histochem. Cell Biol 106:19-30.

Tretter V, Ehya N, Fuchs K, Sieghart W (1997) Stoichiometry and assembly of a recombinant $GABA_A$ receptor subtype. J Neurosci. 17:2728-2737.

Trimmer J S and Rhodes K J (2004) Localization of voltage-gated ion channels in mammalian brain. Annu Rev Physiol. 66:477-519.

Watanabe M, Maemura K, Kanbara K, Tamayama T, and Hayasaki J (2002) GABA and GABA receptors in the central nervous system and other organs. Int Rev Cytol 213:1-47.

Whittington M A, Traub R D and Jefferys J G (1995) Synchronized oscillations in interneuron networks driven by metabotropic glutamate receptor activation. Nature 373: 612-615.

Wilson M A and McNaughton B L (1993) Dynamics of the hippocampal ensemble code for space. Science 261: 1055-1058.

Wisden W, Laurie D J, Monyer H and Seeberg P H (1992) The distribution of 13 $GABA_A$ receptor subunit mRNAs in the rat brain. 1. Telencephalon, diencephalon, mesencephalon. J Neurosci. 12:1040-1062.

Zola-Morgan S, Squire L R, and Amaral D G (1986) Humanamnesia and the medial temporal region: Enduring memory impairment following a bilateral lesion limited to field CA1 of the hippocampus. J Neurosci. 6: 2950-2967.

7. FIGURES AND TABLES

Fig.1 Distribution of immunoreactivity with newly generated antibodies to the α1 and β3 subunits in the hippocampus

(A) The antiserum to the α1 antibody raised in rat produced labeling in the whole hippocampus, the cell body layers, stratum lucidum and the hilus were lightly stained. (B) Some of interneurons (arrows) in the CA3 area are more strongly labeled than neighboring pyramidal cells. (C) The immunolabeling for the β3 subunits was also distributed throughout the hippocampus; the cell body layers, str. lucidum and the hilus were lightly labeled. Scale bar in A = 2.0 mm for A, C; bar in B = 200 μm.

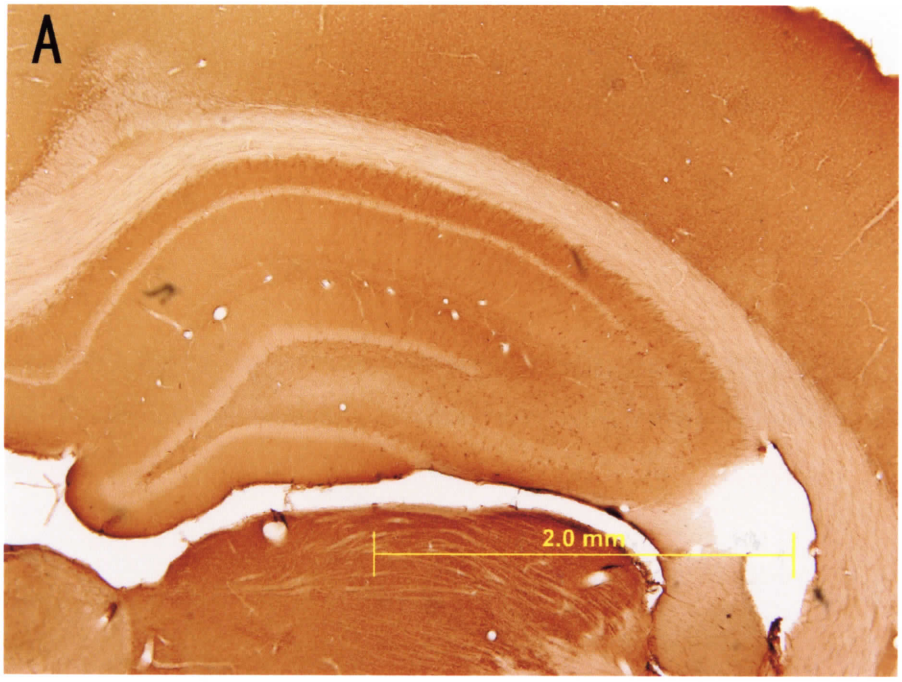
A
2.0 mm

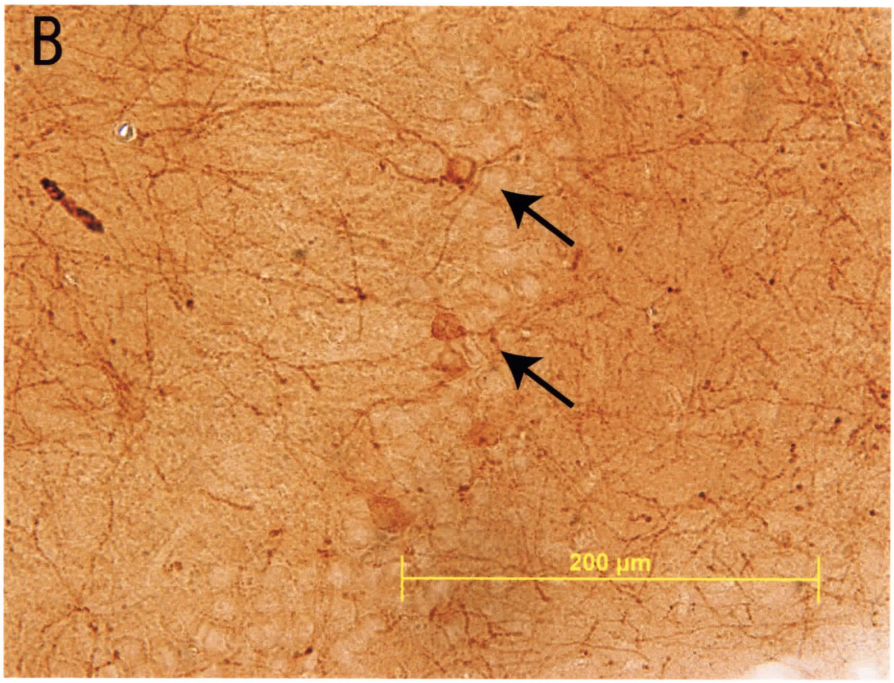
B
200 µm

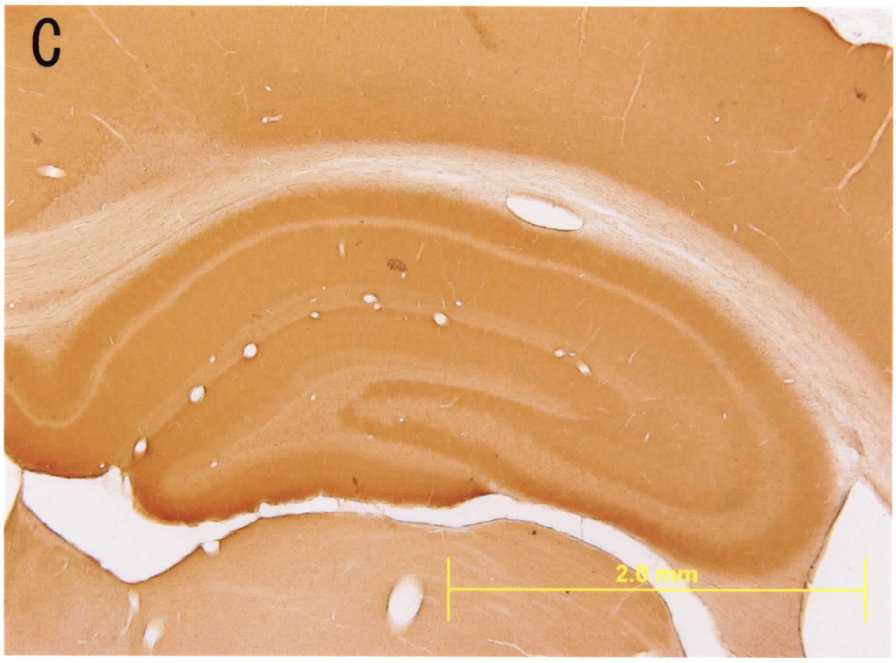
C
2.0 mm

Fig.2 Imunohistchemistry for $GABA_A$ receptor subunits in HEK cells

(A) The antiserum to the β3 subunit raised in guinea pig produced labeling in the HEK cells transfected with β3 subunit, but the antiserum to the α1 antibody in rabbit did not. (B) The HEK cells transfected with α1 subunit are labeled with α1 antiserum raised in rat, but not with the antiserum to the β3 subunit. (C) The HEK cells transfected with α1 subunit are labeled with α1 antiserum raised in rabbit, but not with the antiserum to the β3 subunit. Scale bar = 50 μm.

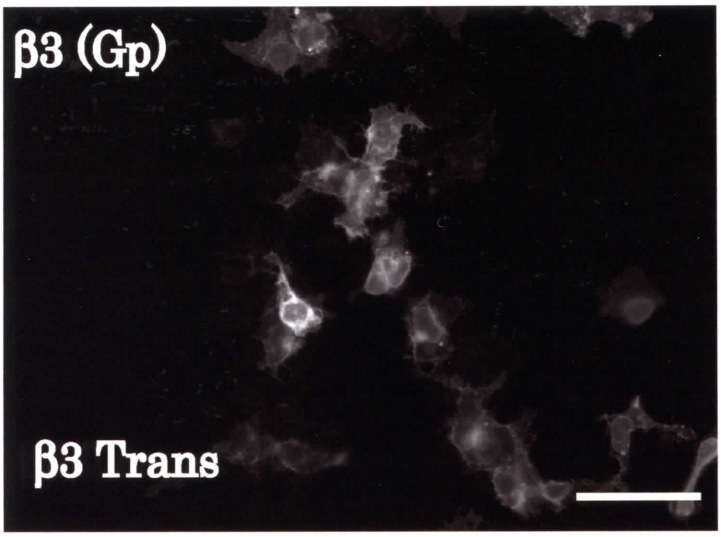
β3 (Gp)
β3 Trans

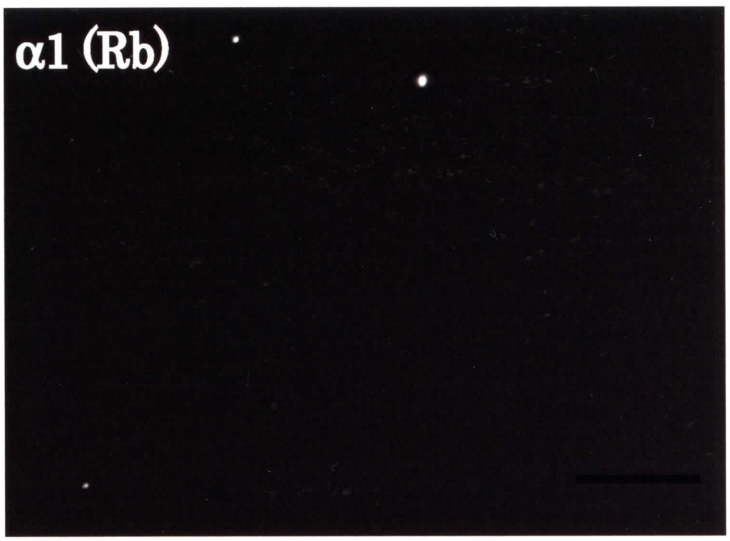
α1 (Rb)

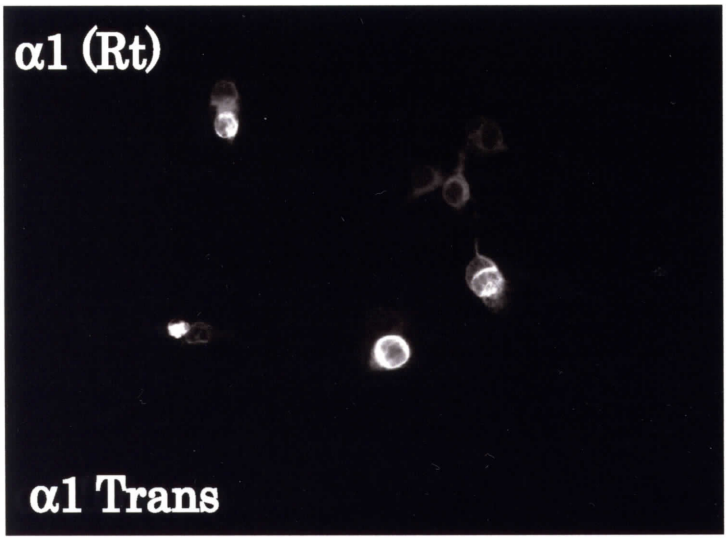
α1 (Rt)
α1 Trans

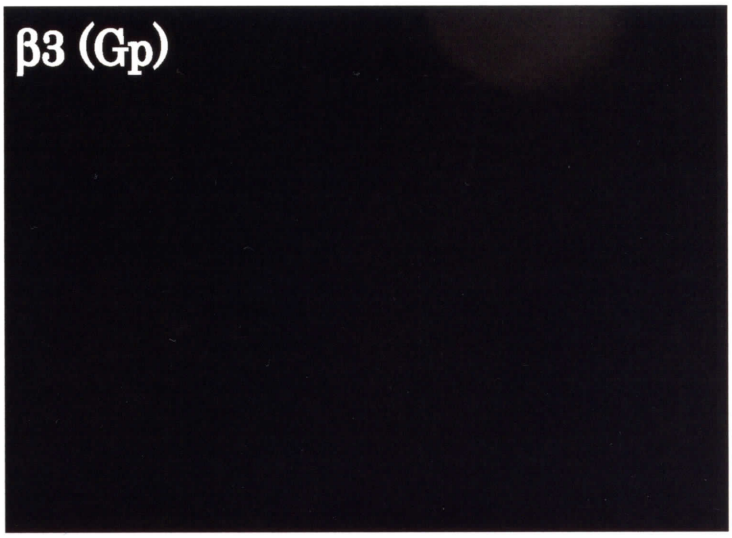
β3 (Gp)

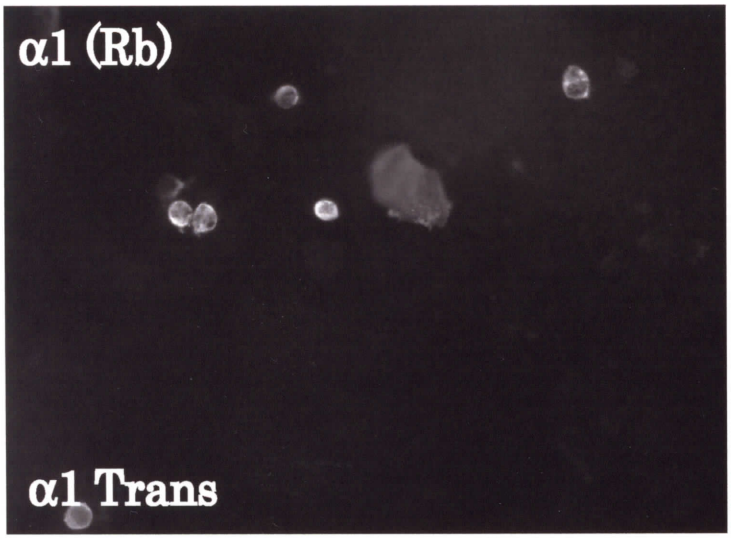
α1 (Rb)
α1 Trans

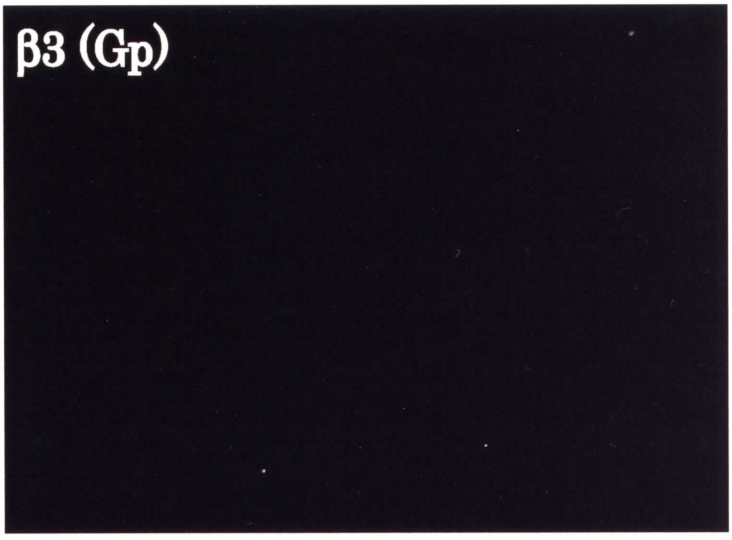
β3 (Gp)

Fig.3 Morphological characteristics of CA1 pyramidal cells in hippocampal replica

(A) A coronal slice of the rat hippocampus. Red frame delineates the area studied in replicas. Ori: stratum oriens, Pyr: stratum pyramidale, Rad: stratum radiatum and Lac: stratum lacunosum moleculare. (B) A replica of the CA1 area is mounted on an electron microscopic grid. The pyramidal cell layer (Pyr) is seen as well as the apical dendrites (arrows) oriented radially. (C, D) Low magnification electron microscopic images of pyramidal somata (Soma) and apical dendrites (Dendrite) are recognized from their position and size. (E) Light microscopic immunoperoxidase labeling for the Nav1.6 subunit of the sodium channel. Because the AIS could not be recognized only from its morphology in replica, we used antibodies to the Nav1.6 subunit as a marker. The dense labeled band of radial short processes at the oriens side of the pyramidal layer (Pyr) shows the AISs. (F) The P-face of an AIS is labeled with the anti-Nav1.6 antibody recognizing an intracellular epitope. Arrows indicates 15 nm gold particles. Scale bar in A = 1.0 mm; bar in B = 200 μm; bar in C and D = 10 nm; bar in E = 200 μm; bar in F = 100 nm.

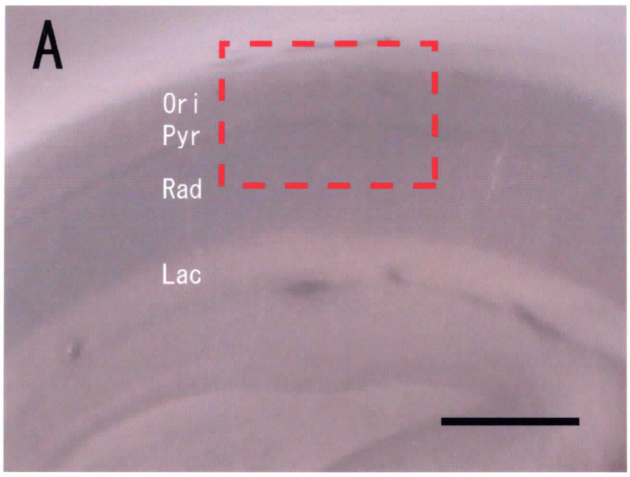
A
Ori
Pyr
Rad
Lac

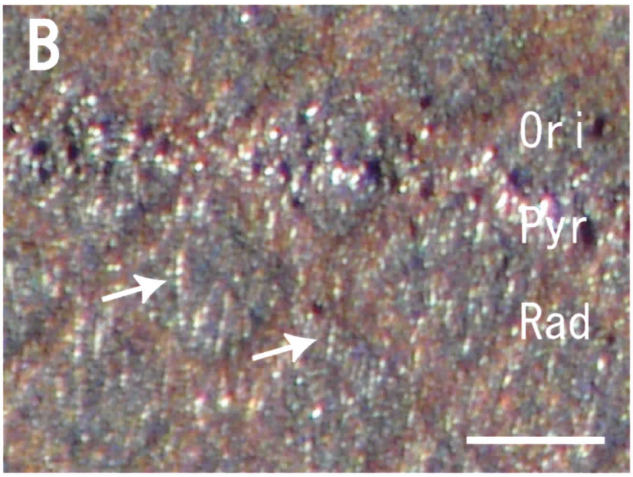
B
Ori
Pyr
Rad

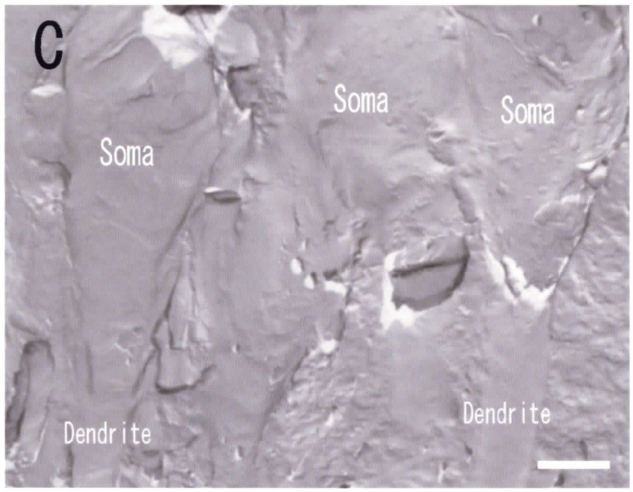
C
Soma
Soma
Soma
Dendrite
Dendrite

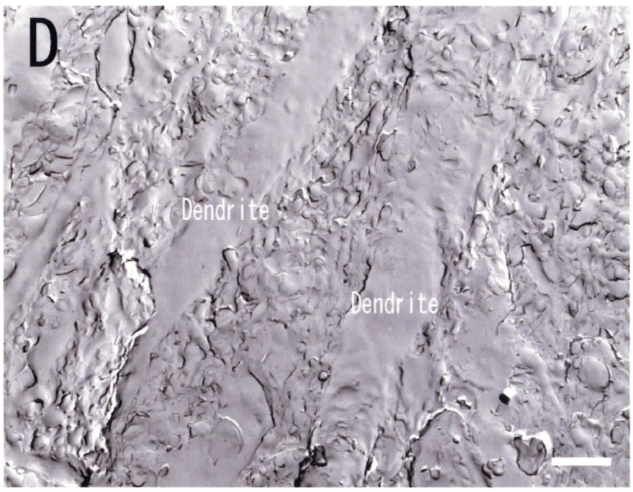
D
Dendrite
Dendrite

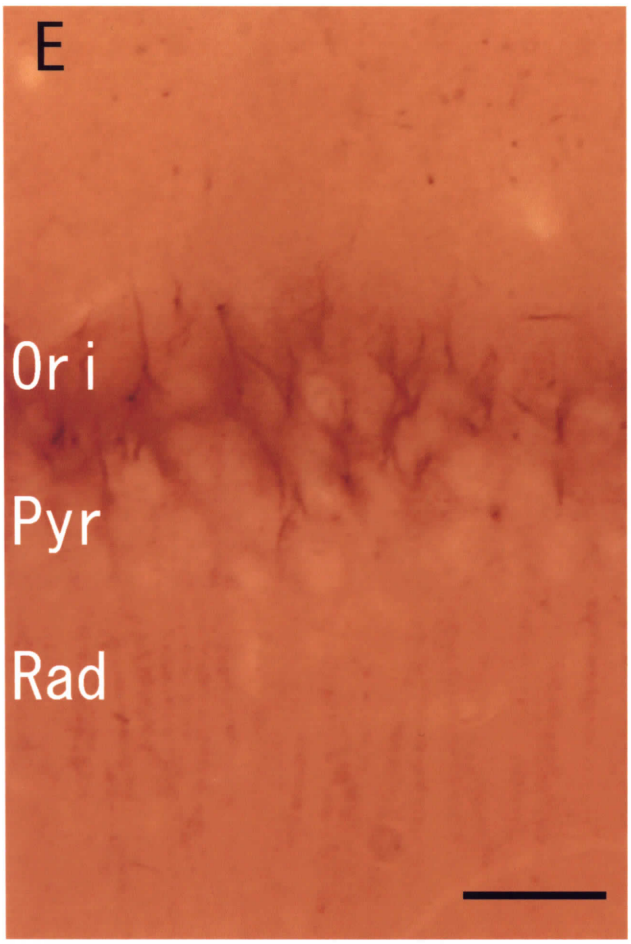
E
Ori
Pyr
Rad


F

Fig.4 The appearance of somatic synapses in the P-face replica and immunolabeling for $GABA_A$ receptor subunits

The IMPs were scattered throughout the P-face, but some formed dense islands. (A) Labeling for the α1 subunit on one (arrow) but not on a second (double arrow) IMP cluster nearby. (B, C) High IMP density is labeled for the α2 (B) and β3 subunits(C), respectively. There is a high correlation of immunogold density for the $GABA_A$ subunits and IMP density, but there is also occasional immunolabeling outside the high IMP density areas. Scale bar = 100 nm.

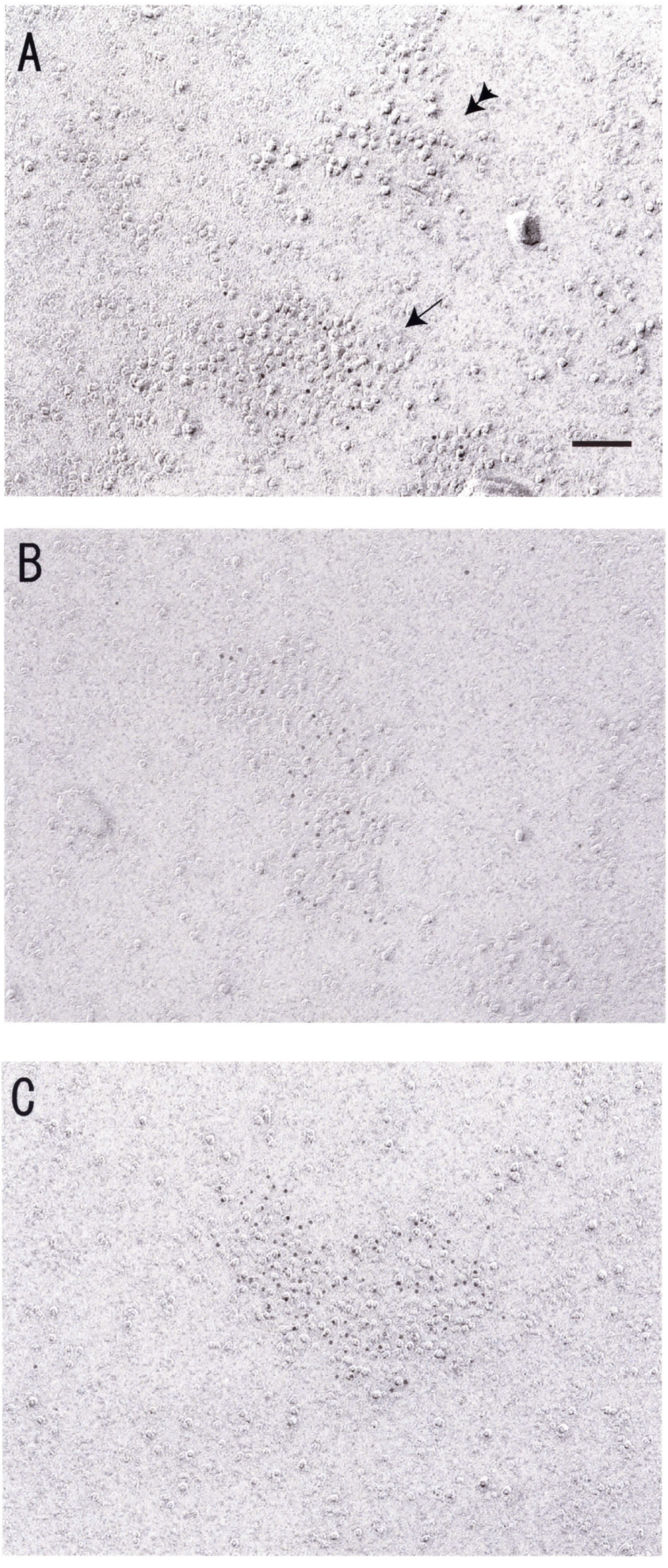
A
B
C

Fig.5 Freeze-fracture immunolabeling for α1 KO and α2 KO mouse

(A) Labeling with α1 antibody (5 nm particles) from rat and β3 antibody (10 nm particles) from Gp on a WT mouse. (B) Labeling with α2 antibody (5 nm particles) from rat and β3 antibody (10 nm particles) from Gp on a WT mouse. (C, E) Labeling with α1 and β3 (C), and with α1 and α2 (E) in α1 KO mouse. (D, F) Labeling with α2 and β3 (D), and with α2 and α1 (E) in α2 KO mouse. The labelings to α1 subunit disappear in α1 KO, and the labelings to α2 subunit in α2 KO. Scale bar = 100nm.

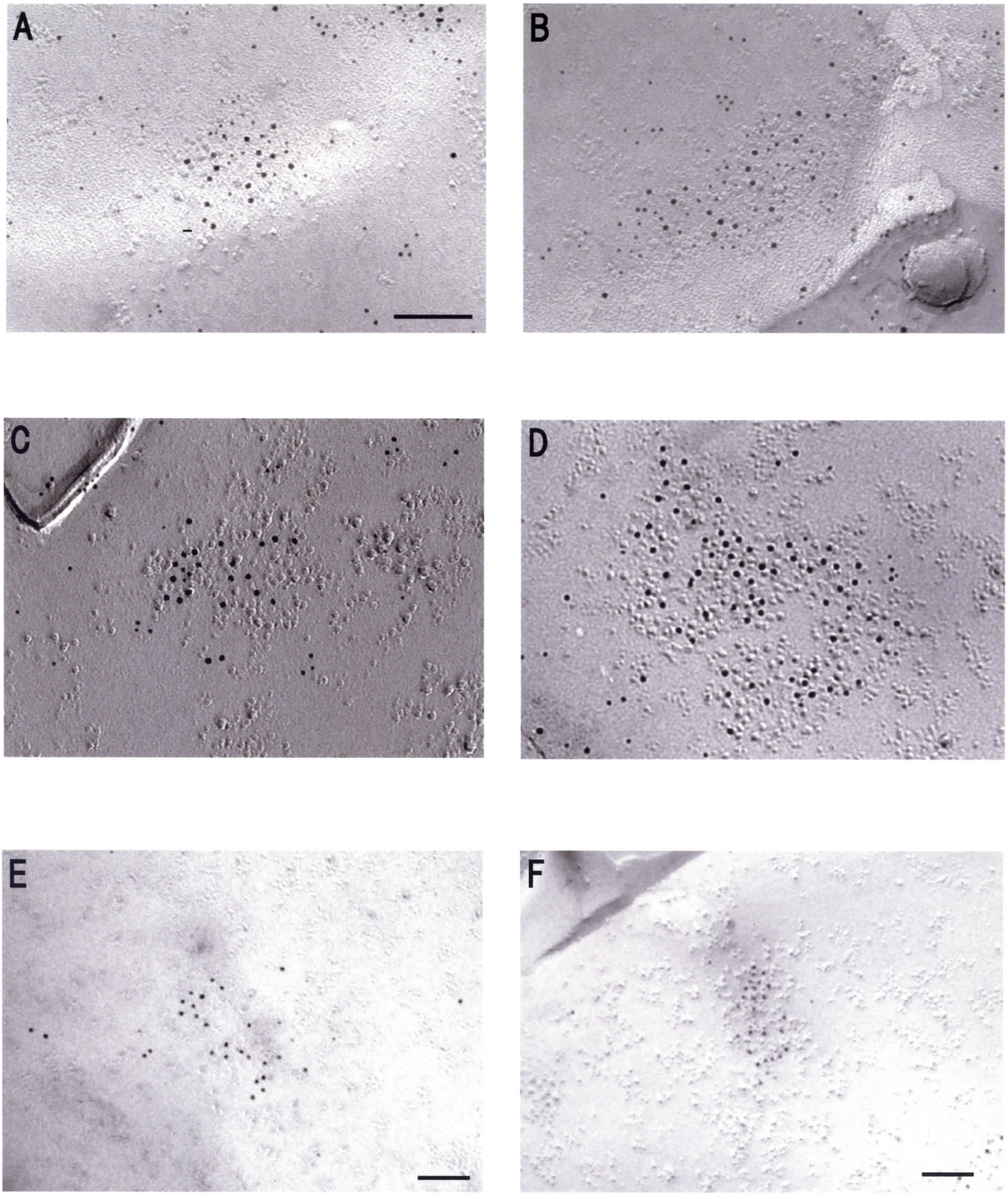
A
B
C
D
E
F

Fig. 6 Synaptic area sizes on the somata of CA1 pyramidal cells obtained in replicas

(A) Distribution of synaptic areas (high density IMP clusters) obtained in the samples taken for measuring immunolabeling for the α1, α2 and β3 subunits. (B) Comparison of sizes (mean ± SD) of the somatic synapse populations labeled for the α1, α2 and β3 subunits. The three samples were not different (Kruskal-Wallis ANOVA test, $p > 0.05$).

A

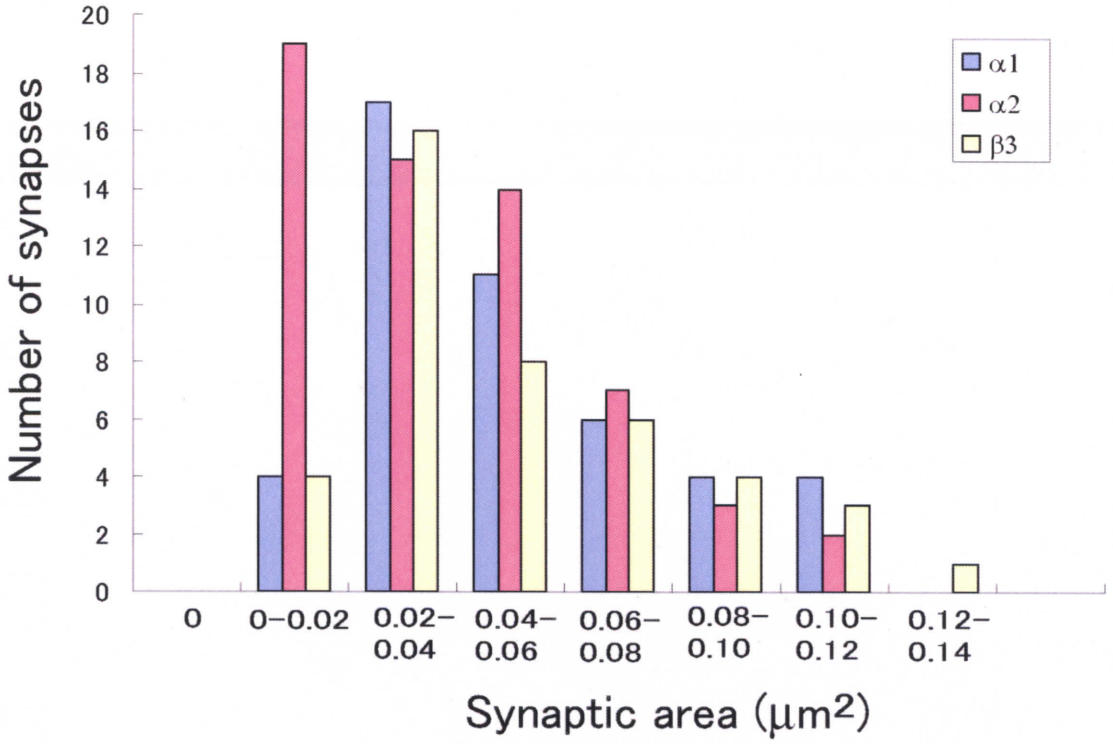
Distribution of labeled IMP area on soma
Number of synapses
20
18
16
14
12
10
8
6
4
2
0
α1
α2
β3
0
0–0.02
0.02–0.04
0.04–0.06
0.06–0.08
0.08–0.10
0.10–0.12
0.12–0.14
Synaptic area (μm2)

B

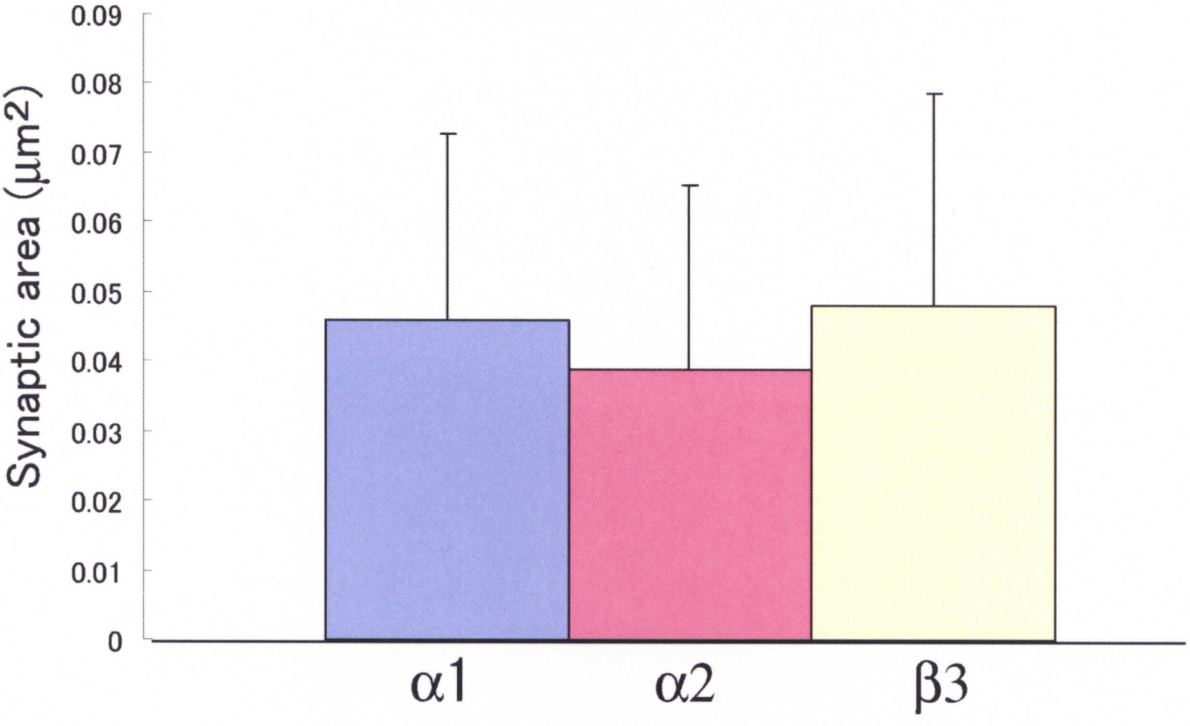
Labeled IMP area on soma
Synaptic area (μm2)
0.09
0.08
0.07
0.06
0.05
0.04
0.03
0.02
0.01
0
α1
α2
β3

Fig. 7 Labeling for the β3 subunits on distinct subcellular compartments of pyramidal cells

(A-D) Examples of labeled synaptic area on a soma (A), an apical dendrite (B) and an AIS (C, D) respectively. The IMP density clusters are labeled with 5 nm gold particles (arrow) for the β3 subunit. The surrounding area in (C) is labeled with 15 nm gold particles (double arrow) for Nav1.6. A synaptic area in (C) is shown in a higher magnification in (D). Scale bar = 100 nm.

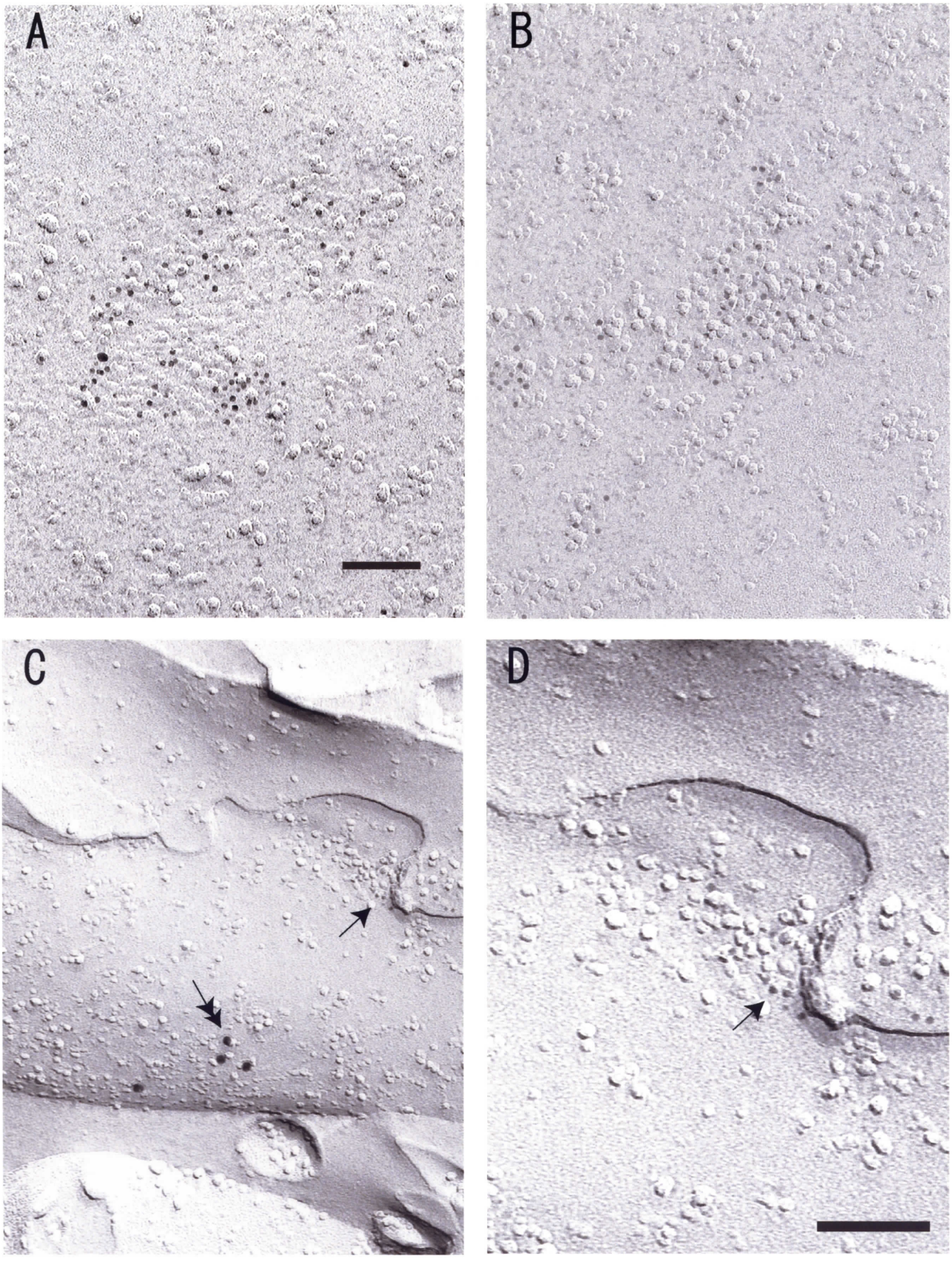
A
B
C
D

Fig. 8 Relationship between number of gold particles for the β3 subunits and synaptic area in the three subcellular compartments

(A) On dendrites and somata the amount of receptor is linearly related to synaptic area. Synapses on AIS were too few for evaluation. (B) Distribution of synaptic areas labeled for β3 in soma, dendrite and AIS. (C) Distribution of immunogold densities in soma, dendrite and AIS. (D) Comparison of labeling density of synaptic (Synapse) and extrasynaptic (Extra) plasma membrane on three subcellular compartments. There was no difference between the three compartments, although the axon initial segment population was small.

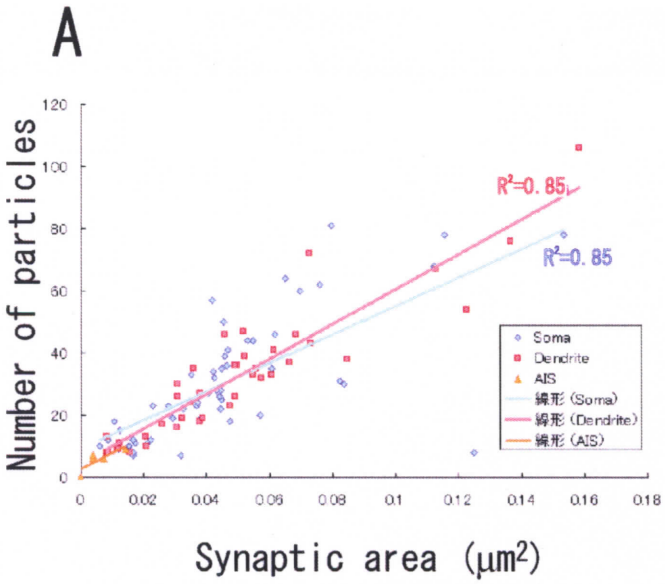
A
Number of particles
Synaptic area (μm2)
R2=0.85
R2=0.85
Soma
Dendrite
AIS
線形 (Soma)
線形 (Dendrite)
線形 (AIS)

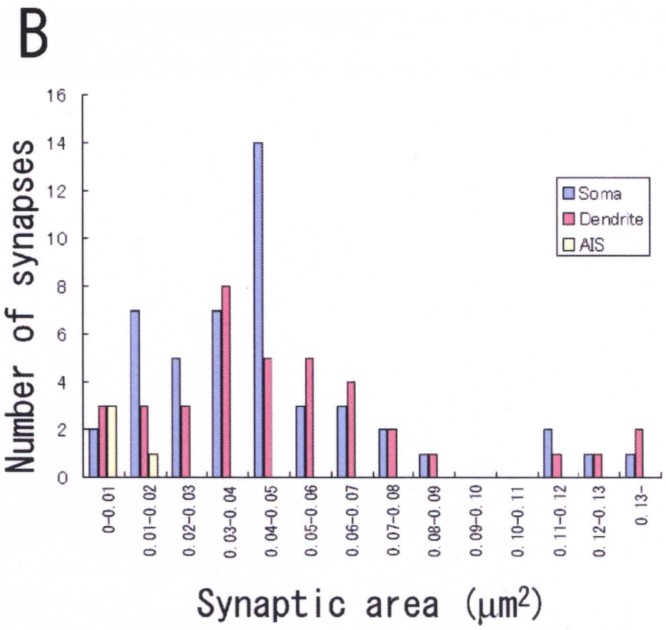
B
Number of synapses
Synaptic area (μm2)
Soma
Dendrite
AIS
0-0.01
0.01-0.02
0.02-0.03
0.03-0.04
0.04-0.05
0.05-0.06
0.06-0.07
0.07-0.08
0.08-0.09
0.09-0.10
0.10-0.11
0.11-0.12
0.12-0.13
0.13-

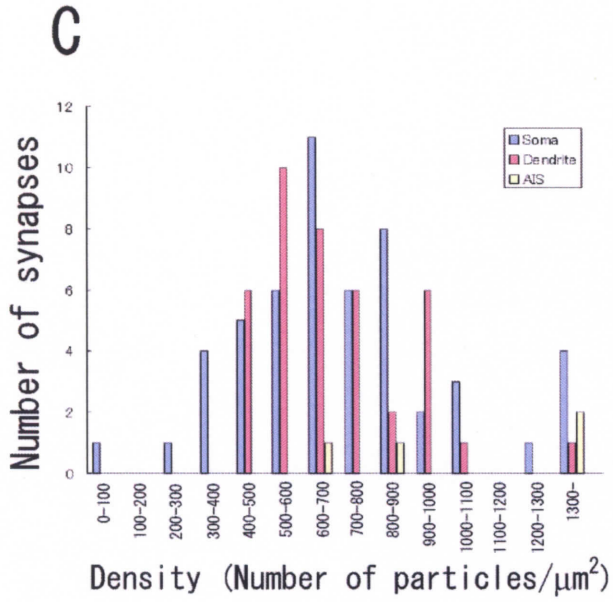
C
Number of synapses
Density (Number of particles/μm2)
Soma
Dendrite
AIS
0-100
100-200
200-300
300-400
400-500
500-600
600-700
700-800
800-900
900-1000
1000-1100
1100-1200
1200-1300
1300-

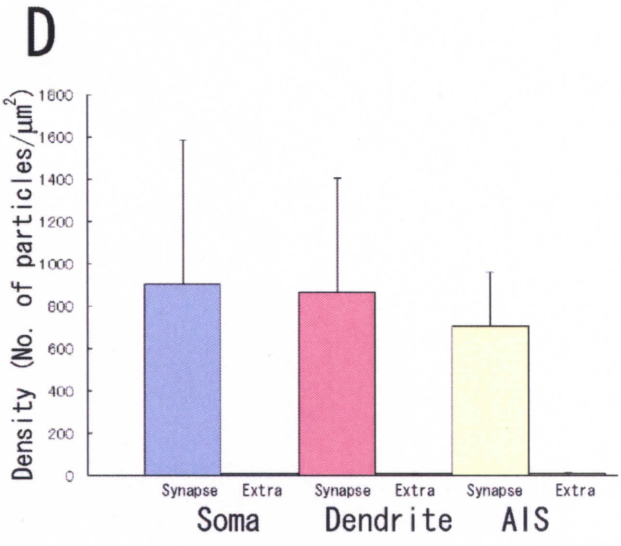
D
Density (No. of particles/μm2)
Synapse
Extra
Soma
Dendrite
AIS

Fig. 9 Labeling for the α1 subunit on distinct subcellular compartments of pyramidal cells

(A, B) Examples of labeled synaptic area on a soma (A) and an apical dendrite (B). Extrasynaptic area on an AIS labeled for α1 (arrows) is shown in low (C) and high (D) magnifications. Double arrow indicates labeling for Nav1.6. Scale bar = 100 nm.

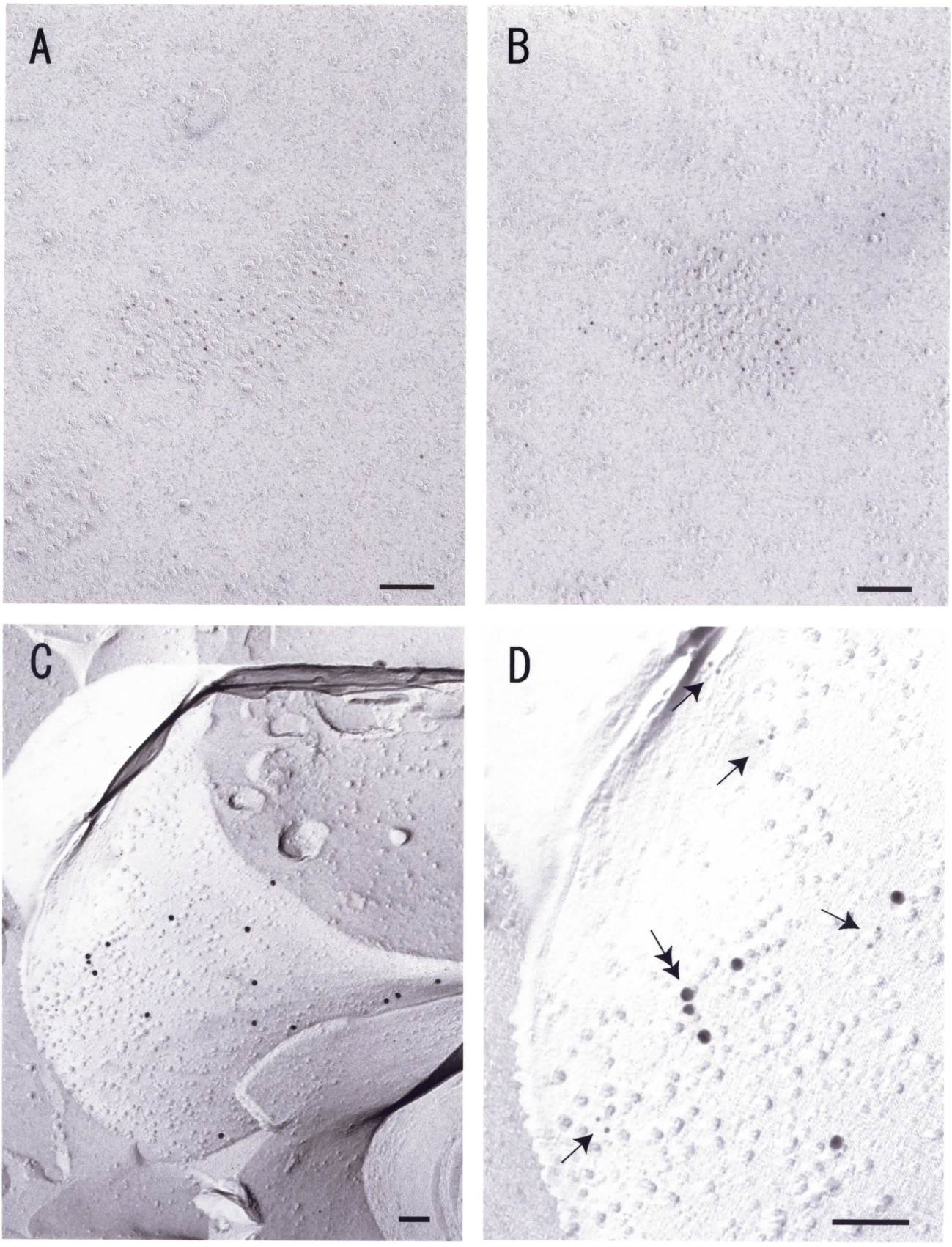
A
B
C
D

Fig. 10 Relationship between number of gold particles for the α1 subunit and synaptic area in two subcellular compartments

(A) On dendrites and somata the amount of receptor is linearly related to synaptic area. In this sample, no synapses were found on AISs. (B) Distribution of synaptic areas labeled for α1 in soma and dendrite. (C) Distribution of immunogold particle densities in soma and dendrite. (D) Comparison of labeling density of synaptic (Synapse) and extrasynaptic (Extra) plasma membrane on three subcellular compartments. There was no difference between synapses on somata and dendrites.

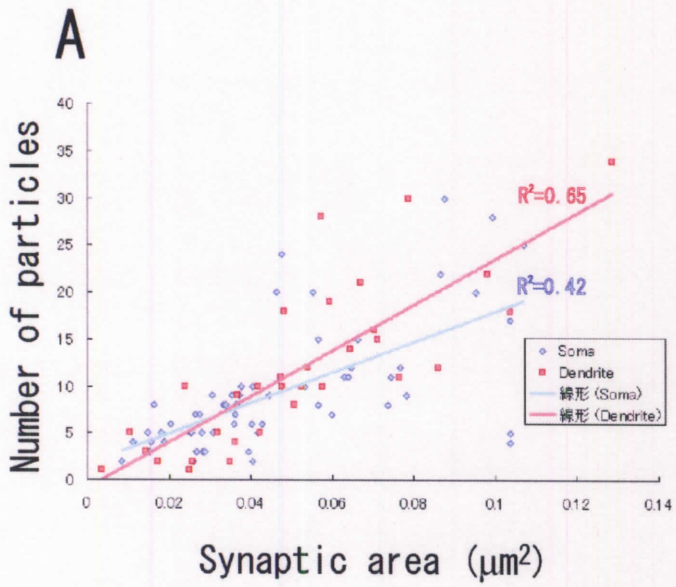
A
Number of particles
Synaptic area (μm2)
R2=0.65
R2=0.42
Soma
Dendrite
線形 (Soma)
線形 (Dendrite)

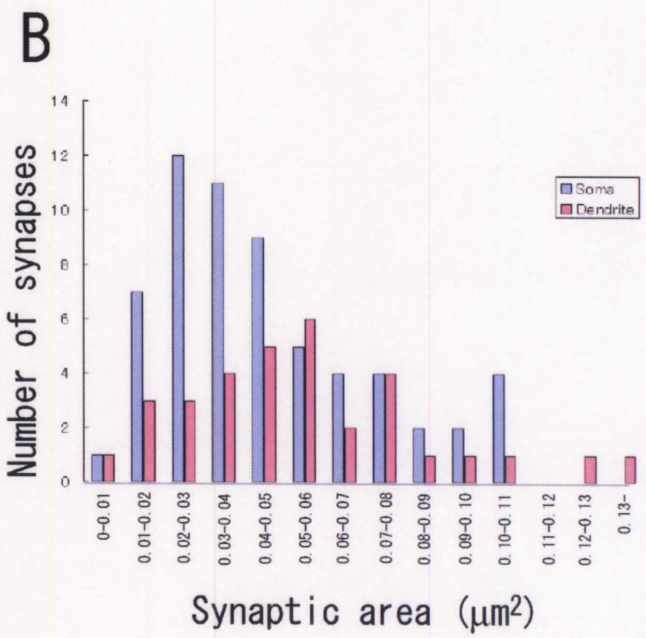
B
Number of synapses
Synaptic area (μm2)
Soma
Dendrite
0-0.01
0.01-0.02
0.02-0.03
0.03-0.04
0.04-0.05
0.05-0.06
0.06-0.07
0.07-0.08
0.08-0.09
0.09-0.10
0.10-0.11
0.11-0.12
0.12-0.13
0.13-

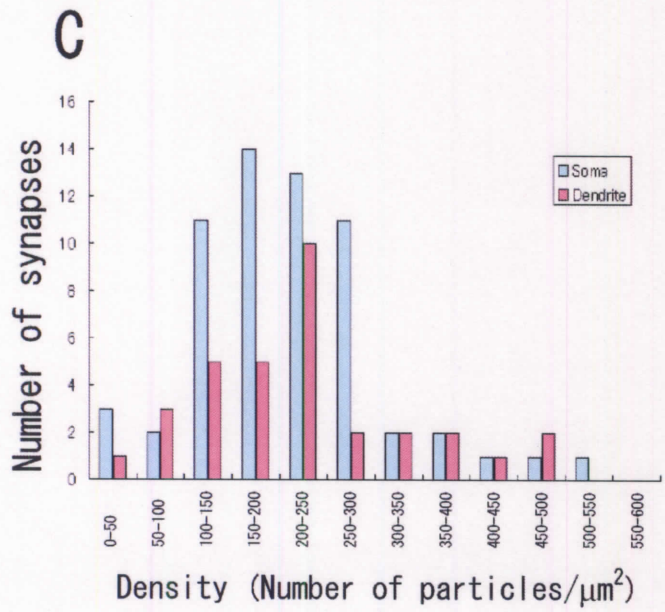
C
Number of synapses
Density (Number of particles/μm2)
Soma
Dendrite
0-50
50-100
100-150
150-200
200-250
250-300
300-350
350-400
400-450
450-500
500-550
550-600

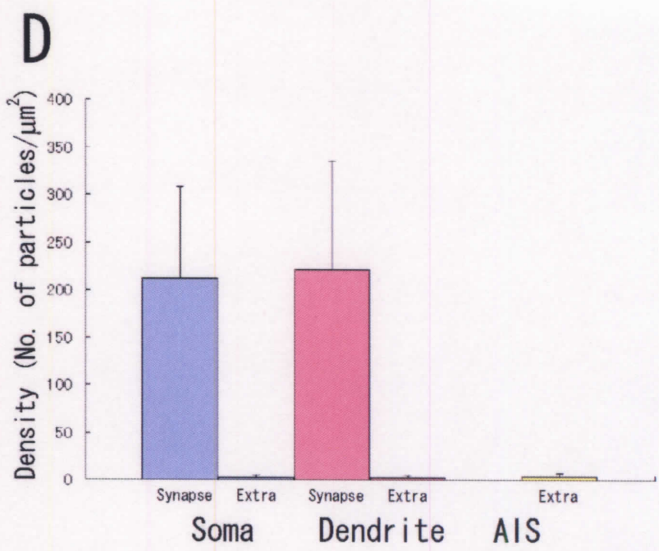
D
Density (No. of particles/μm2)
Synapse
Extra
Synapse
Extra
Extra
Soma
Dendrite
AIS

Fig. 11 Labeling for the α2 subunit on distinct subcellular compartments of pyramidal cells

(A-C) Examples of labeled synaptic area on a soma (A), an apical dendrite (B) and AIS (C, D), respectively. IMP clusters are labeled with 5 nm gold particles (arrows) for the α2 subunit. A synaptic area in (C) is shown in higher magnification in (D). The surrounding area is labeled with 15 nm gold particles (double arrows) for Nav1.6. Scale bar = 100 nm.

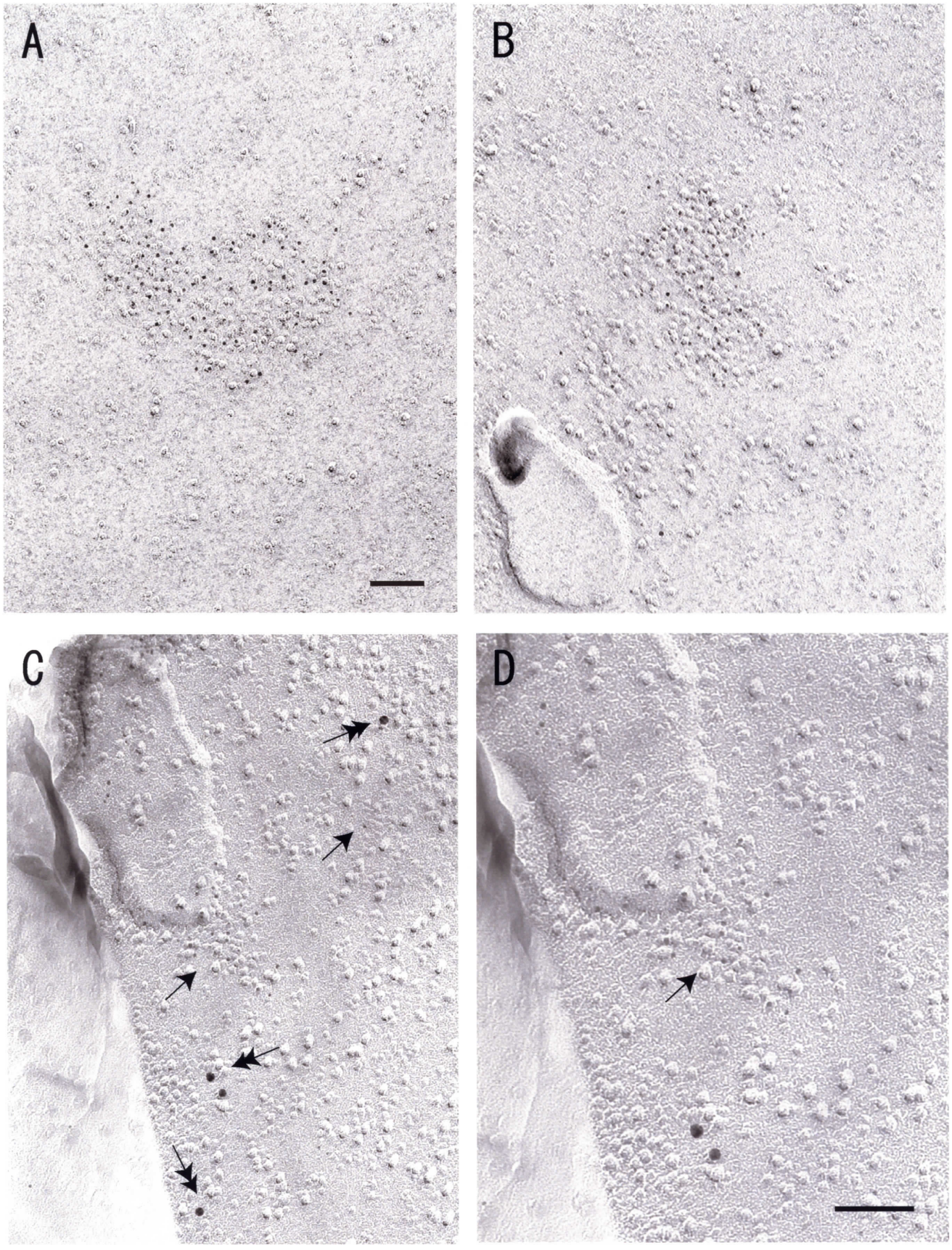
A
B
C
D

Fig. 12 Relationship between number of gold particles for the α2 subunit and synaptic area in the three subcellular compartments

(A) On dendrites and somata the amount of receptor is linearly related to synaptic area, and there is a correlation of the amount of receptor with synaptic area also on the AISs. (B) Distribution of synaptic areas labeled for the α2 subunit in the three subcellular compartments. (C) Distribution of immunogold particle densities in soma, dendrite and AIS. (D) Comparison of labeling density of synaptic (Synapse) and extrasynaptic (Extra) plasma membrane on three subcellular compartments. There was no difference between the three compartments, although the axon initial segment population was small.

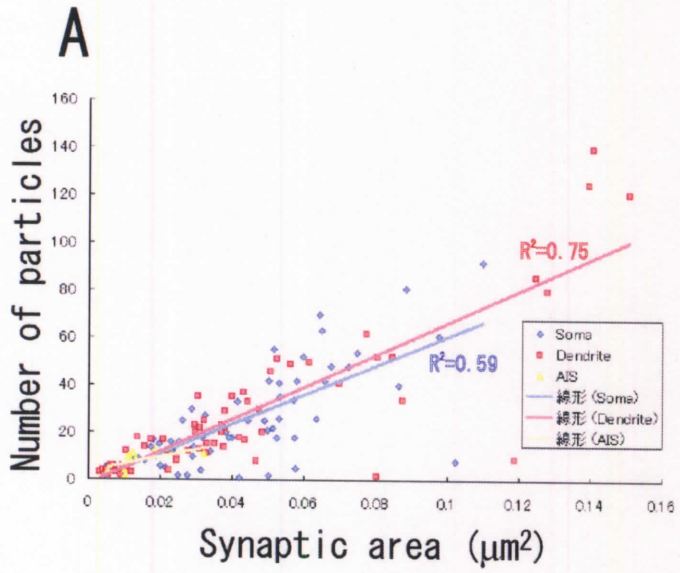
A
Number of particles
Synaptic area (μm2)
R2=0.75
R2=0.59
Soma
Dendrite
AIS
線形 (Soma)
線形 (Dendrite)
線形 (AIS)

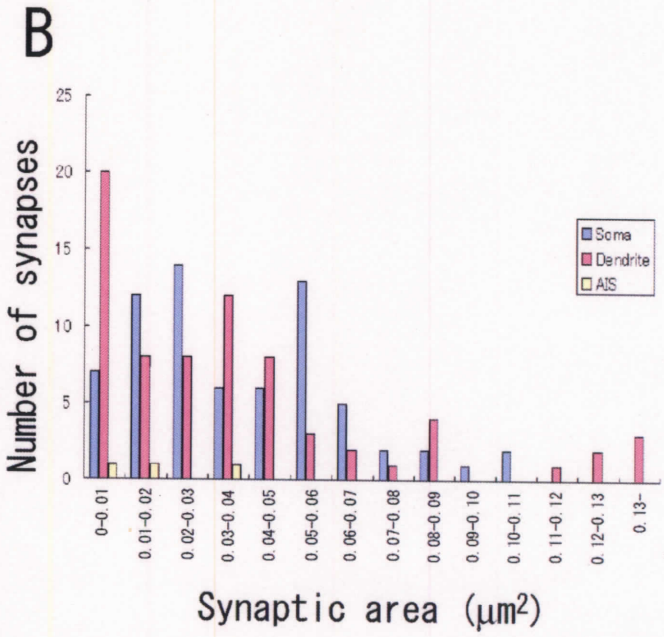
B
Number of synapses
Synaptic area (μm2)
Soma
Dendrite
AIS
0-0.01
0.01-0.02
0.02-0.03
0.03-0.04
0.04-0.05
0.05-0.06
0.06-0.07
0.07-0.08
0.08-0.09
0.09-0.10
0.10-0.11
0.11-0.12
0.12-0.13
0.13-

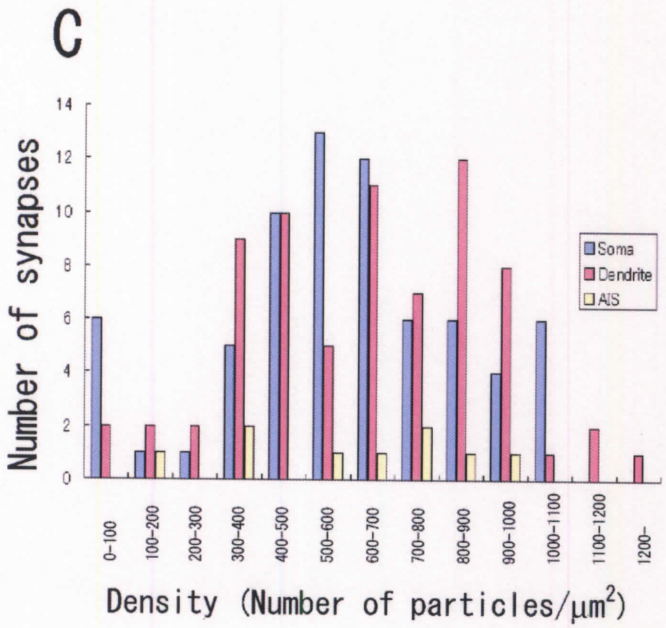
C
Number of synapses
Density (Number of particles/μm2)
Soma
Dendrite
AIS
0-100
100-200
200-300
300-400
400-500
500-600
600-700
700-800
800-900
900-1000
1000-1100
1100-1200
1200-

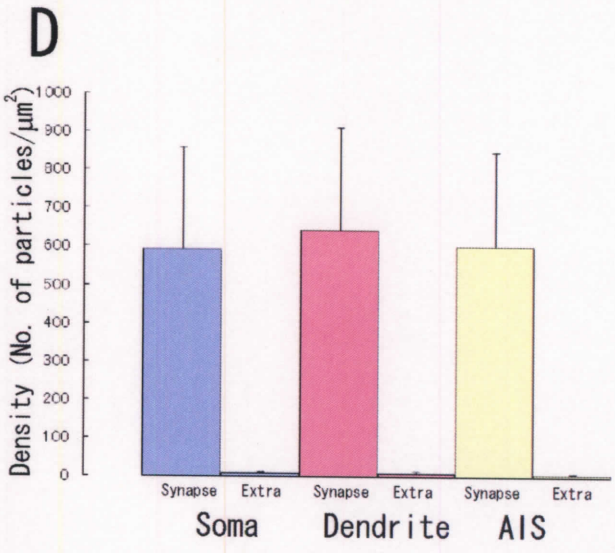
D
Density (No. of particles/μm2)
Synapse
Extra
Soma
Dendrite
AIS

Fig. 13 Synaptic area and receptor subunit distribution in three distinct subcellular compartments of CA1 pyramidal cells

(A-C) The synaptic areas on soma are similar to that on the apical dendrite, but they are both about 3-4 times larger than those on AIS. The sample of dendritic synapses obtained from the replica reacted for the α2 subunit has a significantly smaller size from the other two samples as seen most clearly in the cumulative probability plot in (C) and was also shown by a statistical test (Kruskal-Wallis ANOVA with posthoc Dun test, $p < 0.05$). (B) Cumulative probability plot showing synaptic areas in soma labeled for α1, α2 and β3. (D) The ratios of synaptic to extrasynaptic labeling density are similar for the α1, α2 and β3 subunits and on dendrites and somata. The axon initial segment population was relatively small for detailed comparison.

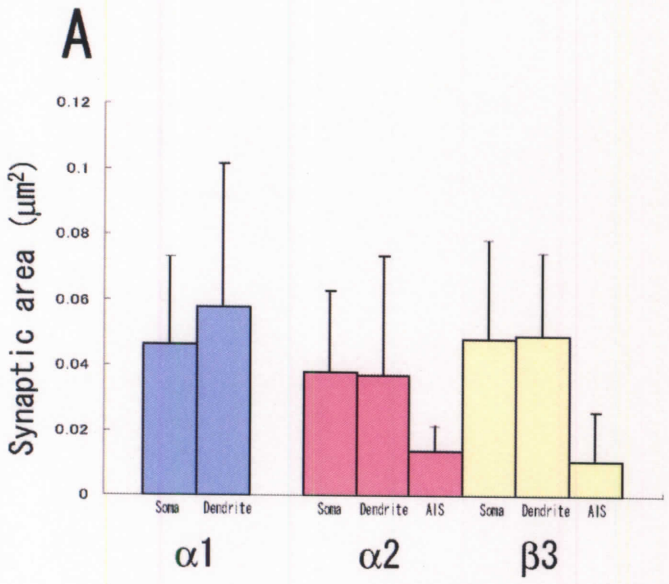
A
Synaptic area (μm²)
0.12
0.1
0.08
0.06
0.04
0.02
0
Soma
Dendrite
Soma
Dendrite
AIS
Soma
Dendrite
AIS
α1
α2
β3

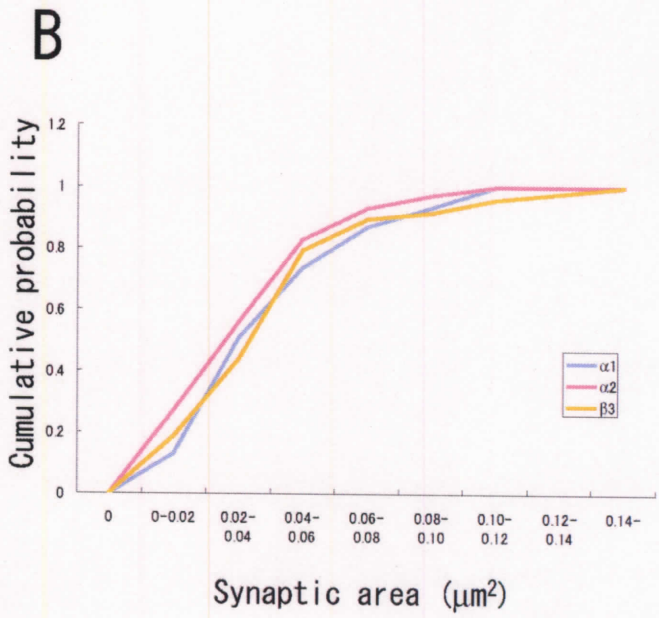
B
Cumulative probability
1.2
1
0.8
0.6
0.4
0.2
0
α1
α2
β3
0
0-0.02
0.02-0.04
0.04-0.06
0.06-0.08
0.08-0.10
0.10-0.12
0.12-0.14
0.14-
Synaptic area (μm²)

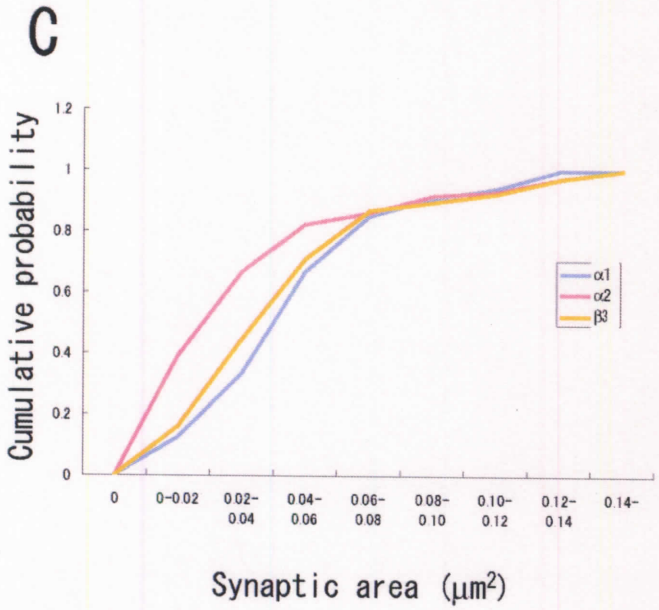
C
Cumulative probability
1.2
1
0.8
0.6
0.4
0.2
0
α1
α2
β3
0
0-0.02
0.02-0.04
0.04-0.06
0.06-0.08
0.08-0.10
0.10-0.12
0.12-0.14
0.14-
Synaptic area (μm²)

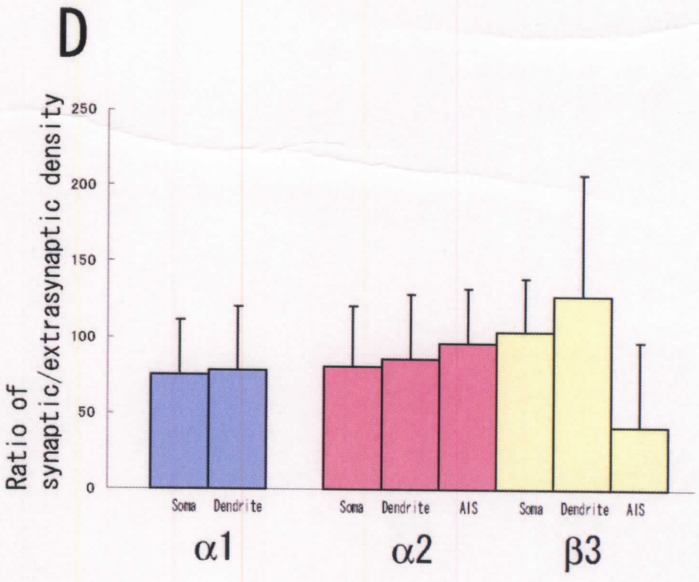
D
Ratio of synaptic/extrasynaptic density
250
200
150
100
50
0
Soma
Dendrite
Soma
Dendrite
AIS
Soma
Dendrite
AIS
α1
α2
β3

Fig. 14 Examples of labeled synaptic areas on somata using antibodies to the α1 and β3 subunits in sequential reactions and switching immunogold sizes

An area of IMP density is labeled with 5 nm gold particles (arrows) for the first primary antibody and with 10 nm gold particles (double arrows) for the second primary antibody. (A) The reaction for α1 antibody is followed by β3 antibody. (B) The reaction for β3 is followed by α1 antibody. Areas indicated by broken lines in (A) and (B) are shown with a higher magnification in (C) and (D), respectively. Scale bar = 100 nm.

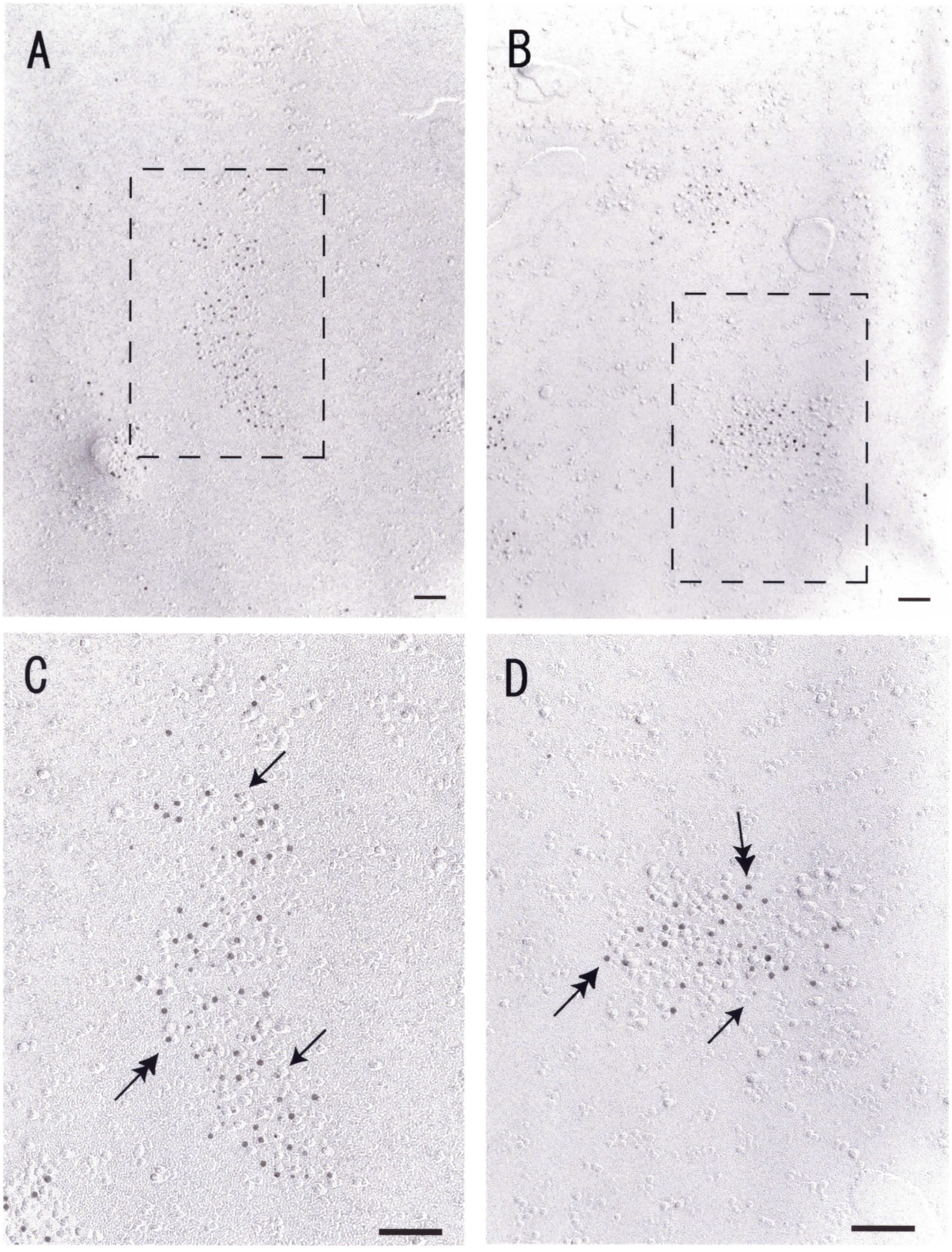
A
B
C
D

Fig. 15 Examples of labeled synaptic areas on somata using antibodies to the α2 and β3 subunits in sequential reactions and switching immunogold sizes

An area of IMP density is labeled with 5 nm gold particles (arrows) for the first primary antibody and with 10 nm gold particles (double arrows) for the second primary antibody. (A) The reaction for α2 antibody is followed by β3 antibody. (B) The reaction for β3 is followed by α2 antibody. Areas indicated by broken lines in (A) and (B) are shown with a higher magnification in (C) and (D), respectively. Scale bar = 100 nm.

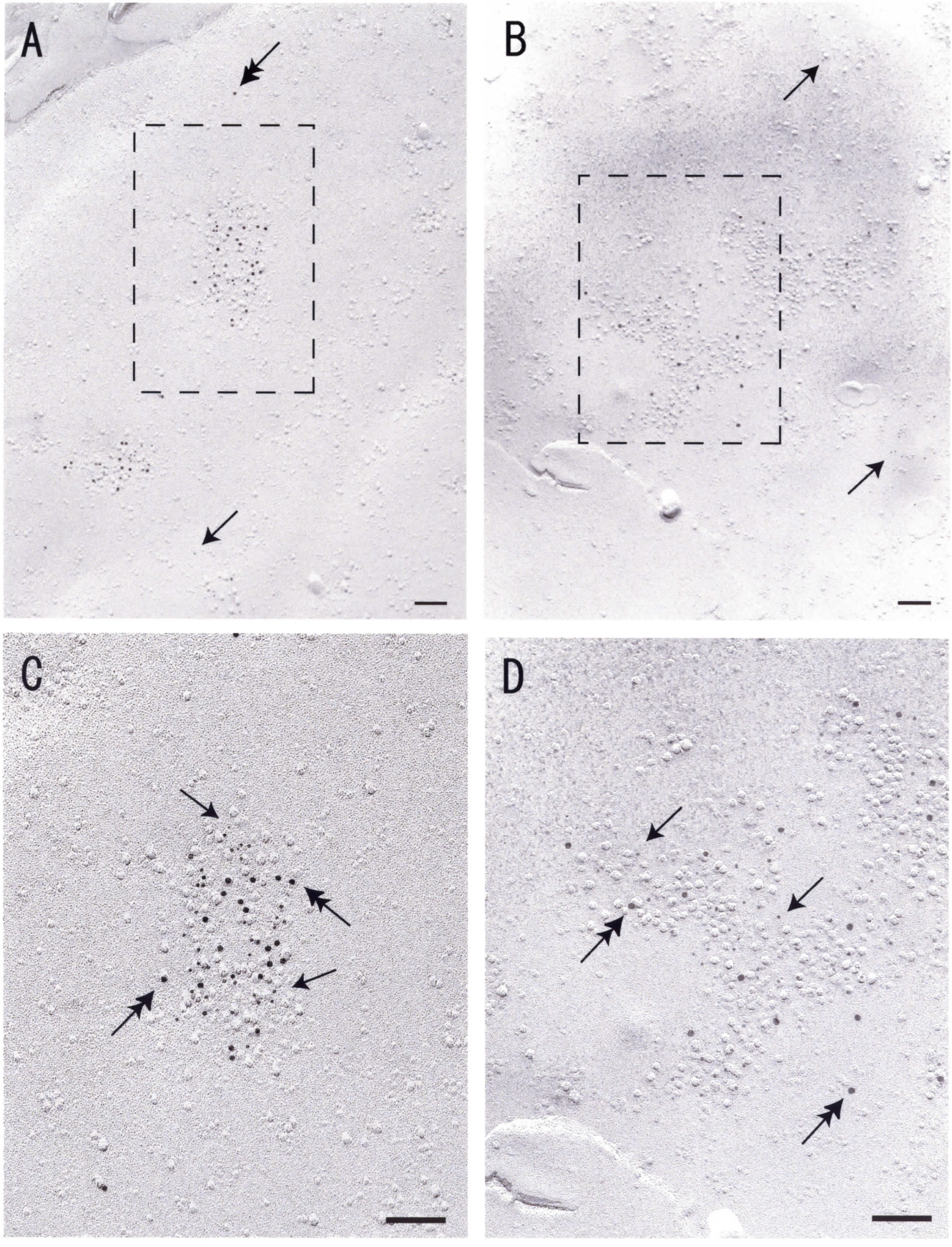
A
B
C
D

Fig. 16 Examples of labeled synaptic areas on somata using antibodies to the α1 and α2 subunits in sequential reactions and switching immunogold sizes

An area of IMP density is labeled with 5 nm gold particles (arrows) for the first primary antibody and with 10 nm gold particles (double arrows) for the second primary antibody. (A) The reaction for α1 antibody is followed by α2 antibody. (B) The reaction for α2 is followed by α1 antibody. Areas indicated by broken lines in (A) and (B) are shown with a higher magnification in (C) and (D), respectively. Scale bar = 100 nm.

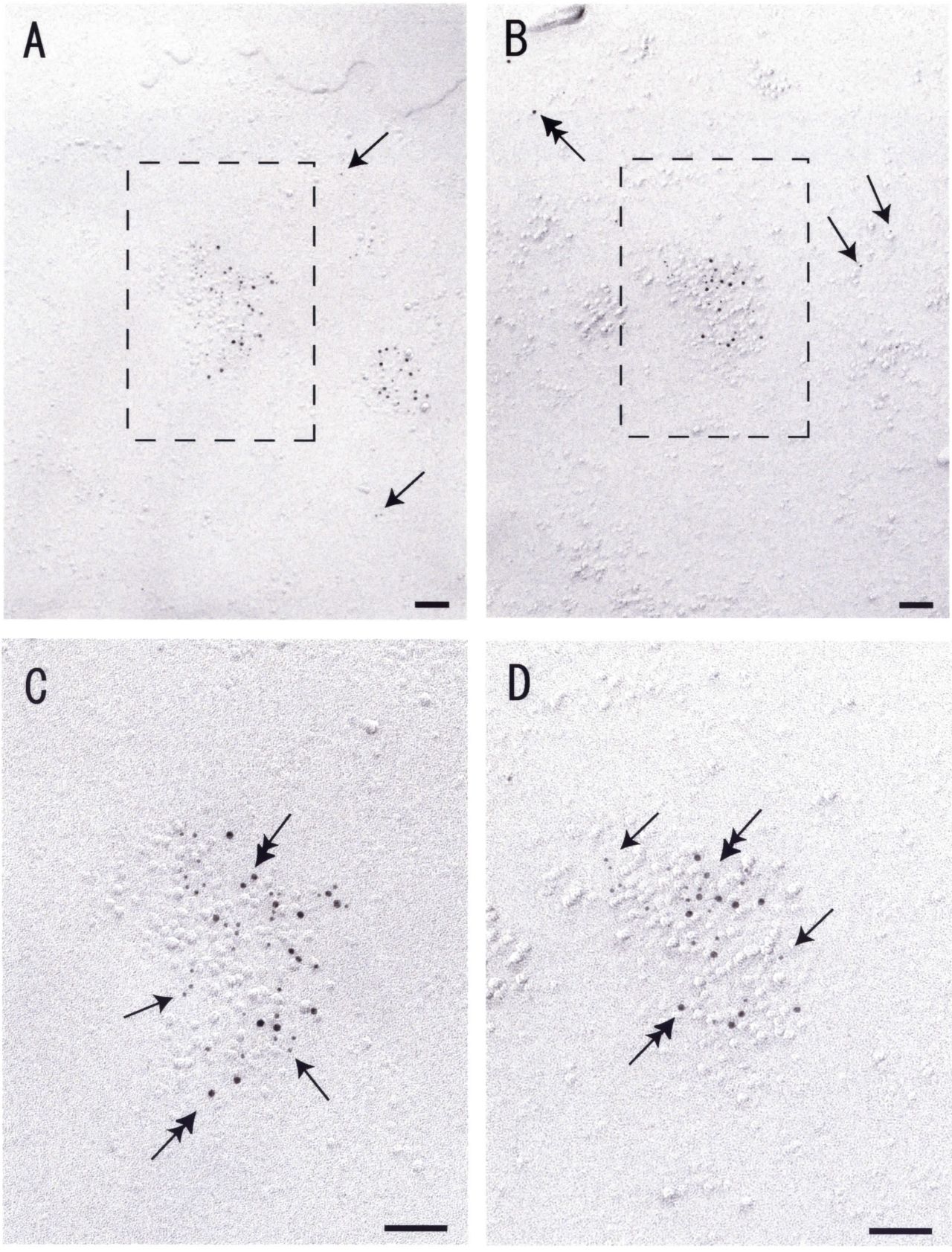
A
B
C
D

Fig. 17 Frequency distributions of synapse sizes for β3, α1 and α2 in double labeled samples

The synaptic area distributions were not normal, but skewed to large values (Shapiro-Wilk test $p < 0.05$). (A) Distributions of synaptic sizes for the β3 subunit. There are no significant difference between double labelings, but distribution in single labeling is shifted to smaller values. Distribution of synaptic sizes for the α1 subunit (B) and α2 subunit (C), respectively.

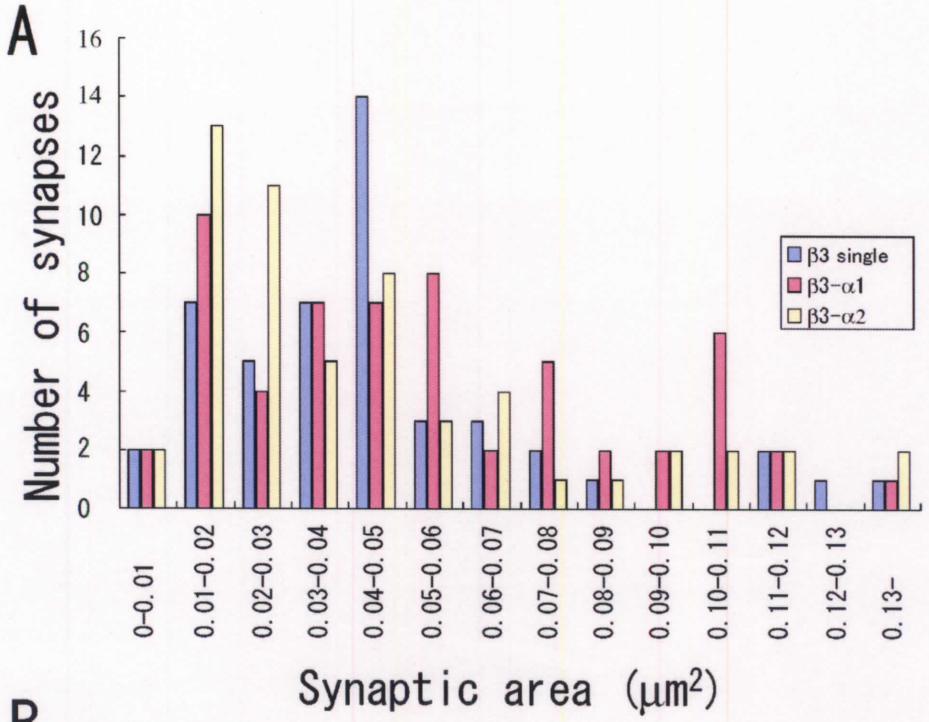
A
Number of synapses
16
14
12
10
8
6
4
2
0
β3 single
β3-α1
β3-α2
0-0.01
0.01-0.02
0.02-0.03
0.03-0.04
0.04-0.05
0.05-0.06
0.06-0.07
0.07-0.08
0.08-0.09
0.09-0.10
0.10-0.11
0.11-0.12
0.12-0.13
0.13-
Synaptic area (μm²)

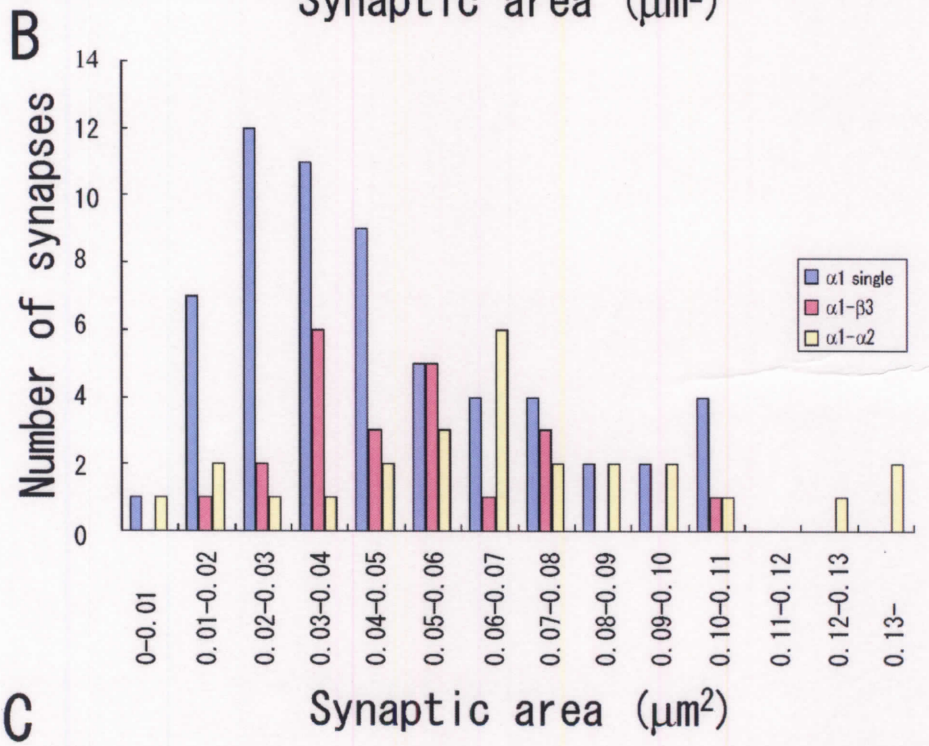
B
Number of synapses
14
12
10
8
6
4
2
0
α1 single
α1-β3
α1-α2
0-0.01
0.01-0.02
0.02-0.03
0.03-0.04
0.04-0.05
0.05-0.06
0.06-0.07
0.07-0.08
0.08-0.09
0.09-0.10
0.10-0.11
0.11-0.12
0.12-0.13
0.13-
Synaptic area (μm²)

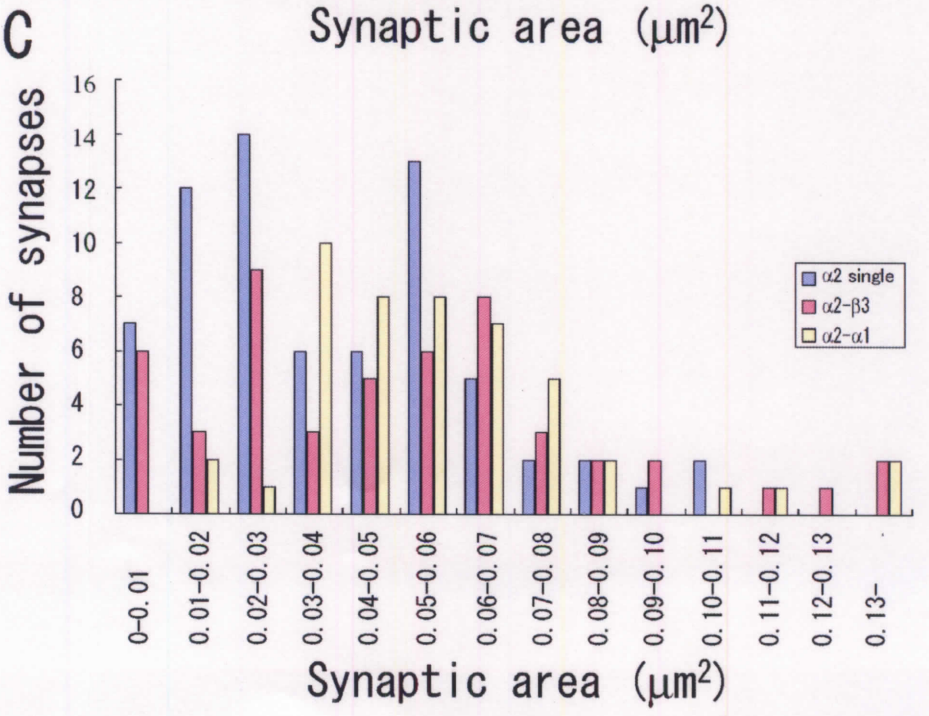
C
Number of synapses
16
14
12
10
8
6
4
2
0
α2 single
α2-β3
α2-α1
0-0.01
0.01-0.02
0.02-0.03
0.03-0.04
0.04-0.05
0.05-0.06
0.06-0.07
0.07-0.08
0.08-0.09
0.09-0.10
0.10-0.11
0.11-0.12
0.12-0.13
0.13-
Synaptic area (μm²)

Table A Antibody specificity as tested on transfected HEK cells

Almost antibodies showed their specificity (only β2 antibody showed weak reaction expressed β1 subunit). Particularly it is very important that the antibodies that I used in this thesis have their own specificity.

Table A

Subunit / Antibodies	α1	α2	α5	β1	β2	β3	γ2
α1 (Rb)	++	−	−	−	−	−	−
α1 (Gp)	+++	−	−	−	−	−	−
α1 (Rt)	+++	−	−	−	−	−	−
α2 (Rb)	−	+++	−				−
α5 (Rb)	−	−	++	−			−
β1 (Rb)		−		+++	−	−	−
β2 (Rb)	−	−		+	+++	−	
β3 (Rb)	−	−	−	−	−	+++	−
β3 (Gp)	−	−	−	−	−	+++	−
γ2 (Rb)		−					++

Rb: Rabbit, Gp: Guinea pig, Rt: Rat

Table B Density of each subunit labeling and synaptic area in distinct subcellular compartments of pyramidal cells

Immunolabeling on the somata, apical dendrites and AISs were compared, and labeled synaptic areas were also compared. The different antibodies to the three subunits produced very similar results.

Table B

	Synaptic area (μm^2)			Synaptic labeling density (No/μm^2)			Extra synaptic labeling density (No/μm^2)			Ratio of synapse/extrasynapse		
	Mean	SD	No. of synapses	Mean	SD	No. of synapses	Mean	SD	No of cells	Mean	SD	No. of synapses
α1 single labeling, Soma	0.046	0.026	61	212.25	96.41	61	2.76	1.16	5	75.3	36.4	61
α1 single labeling, Dendrite	0.058	0.044	33	220.82	113.9	33	2.93	1.41	5	77.8	42.0	33
α1 single labeling, AIS							3.89	3.45	10			
α2 single labeling, Soma	0.038	0.025	70	592.23	267.02	70	7.61	4.16	5	80.6	40.3	70
α2 single labeling, Dendrite	0.037	0.037	72	642.63	269.20	72	7.82	5.42	5	86.0	42.5	72
α2 single labeling, AIS	0.014	0.007	3	601.78	245.45	9	4.70	3.40	10	96.2	36.4	9
β2/3 single labeling, Soma	0.048	0.030	54	904.81	682.08	54	8.00	4.49	5	103.5	35.8	54
β2/3 single labeling, Dendrite	0.049	0.025	35	863.08	542.32	35	7.86	4.13	4	127.3	79.9	35
β2/3 single labeling, AIS	0.011	0.015	4	704.02	254.09	4	7.67	5.50	4	41.0	56.4	4

Table C Co-localization of each subunit on somata of pyramidal cells

These results lead to the conclusion that 80% of β3 positive GABAergic synapses on soma include α1 or α2 subunits, and that α1 subunits and α2 subunits are almost always co-localized in the same synapses.

Table C

	Labeled synapses No. ratio of 1st ab to 2nd ab (%)
α1- β2/3 double labeling	81
β2/3 - α1 double labeling	96
α2- β2/3 double labeling	83
β2/3- α2 double labeling	100
α1- α2 double labeling	97
α2- α1 double labeling	87

8. ACKNOWLEDGEMENTS

First of all, I would like to express my sincere appreciation to Professor Ryuichi Shigemoto for continuous support, encouragements and helpful advice through this study and his patience.

I would like to thank Professor Peter Somogyi for suggesting this project, extending facilities and advices through this study. His lab members' great helps are highly appreciated as well.

I would like to thank Dr. Yugo Fukazawa for advices through this study and for the technical development of SDS-FRL. I also acknowledge for Professor Sieghart and his lab members for providing antibodies and expression plasmids for $GABA_A$ subunits. I am very grateful to Professor McIlhinney and his group for giving cultured cells.

I thank my gratitude to Professor Imoto and his laboratory members for acceptance to join their journal club on every Wednesday morning, which let me learn various works in the field of neuroscience.

My greatest thanks are reserved for my families whose kind supported through over my student live. I have been able to achieve a result as they allow me to do what I'm pleased at.